# A Wearable Tele-Health System towards Monitoring COVID-19 and Chronic Diseases

Wei Jiang, Sumit Majumder, *Graduate Student Member, IEEE*, Samarth Kumar, Sophini Subramaniam, Xiaohe Li, Ridha Khedri, Tapas Mondal, Mansour Abolghasemian, Imran Satia, and M. Jamal Deen, *Fellow, IEEE*

***Abstract*—Severe acute respiratory syndrome coronavirus 2 (SARS-CoV-2) has caused a pandemic since early 2020. The coronavirus disease 2019 (COVID-19) has already caused more than three million deaths worldwide and affected people's physical and mental health. COVID-19 patients with mild symptoms are generally required to self-isolate and monitor for symptoms at least for 14 days in the case the disease turns towards severe complications. In this work, we overviewed the impact of COVID-19 on the patients' general health with a focus on their cardiovascular, respiratory and mental health, and investigated several existing patient monitoring systems. We addressed the limitations of these systems and proposed a wearable telehealth solution for monitoring a set of physiological parameters that are critical for COVID-19 patients such as body temperature, heart rate, heart rate variability, blood oxygen saturation, respiratory rate, blood pressure, and cough. This physiological information can be further combined to potentially estimate the lung function using artificial intelligence (AI) and sensor fusion techniques. The prototype, which includes the hardware and a smartphone app, showed promising results with performance comparable to or better than similar commercial devices, thus potentially making the proposed system an ideal wearable solution for long-term monitoring of COVID-19 patients and other chronic diseases.**

***Index Terms*—COVID-19, SARS-CoV-2, vital signs, wearable monitoring system, telehealth, e-health, chronic diseases, public health, body temperature, heart rate, HRV, SpO2, respiratory rate, blood pressure, cough, Electrocardiogram, ECG, Photoplethysmography, PPG, lung function.**

Manuscript received November 27, 2020; revised March 1, 2021; accepted March 22, 2021. Date of publication March 30, 2021; date of current version January 24, 2022. This work was supported by Canada Research Chair program, NSERC of Canada, and CFI. *(Wei Jiang and Sumit Majumder contributed equally to this work) (Corresponding author: M. Jamal Deen.)*

Wei Jiang and Sophini Subramaniam are with the McMaster School of Biomedical Engineering, McMaster University, Hamilton, ON L8S 4K1, Canada (e-mail: jiangw35@mcmaster.ca; subras1@mcmaster.ca).

Sumit Majumder and Samarth Kumar are with the Electrical and Computer Engineering Department, McMaster University, Hamilton, ON L8S 4K1, Canada (e-mail: majums3@mcmaster.ca; kumars38@mcmaster.ca).

Xiaohe Li is with the The Third People's Hospital of Shenzhen, Guangdong Province, 518112, China (e-mail: little_crane_li@163.com).

Ridha Khedri is with the Computing and Software Department, McMaster University, Hamilton, ON L8S 4K1, Canada (e-mail: khedri@mcmaster.ca).

Tapas Mondal is with Pediatrics, McMaster University, Hamilton, ON L8S 4K1, Canada (e-mail: mondalt@mcmaster.ca).

Mansour Abolghasemian is with Ortho Biomed Inc., Vaughan, ON L4K 0G7, Canada (e-mail: ma@orthobiomed.ca).

Imran Satia is with the Department of Medicine, Division of Respirology, McMaster University, Hamilton, ON L8S 4K1, Canada, and also with Firestone Institute for Respiratory Health, St Joseph's Healthcare, Hamilton, ON L8S 4K1, Canada (e-mail: satiai@mcmaster.ca).

M. Jamal Deen is with the McMaster School of Biomedical Engineering, McMaster University, Hamilton, ON L8S 4K1, Canada, and also with the Electrical and Computer Engineering Department, McMaster University, Hamilton, ON L8S 4K1, Canada (e-mail: jamal@mcmaster.ca).

Digital Object Identifier 10.1109/RBME.2021.3069815

## I. INTRODUCTION

MILLIONS of individuals have been infected by severe acute respiratory syndrome coronavirus 2 (SARS-CoV-2). The global death toll due to SARS-CoV-2 infection or "coronavirus disease 2019" (COVID-19) has already exceeded three million [1]. This virus affects the physical health of individuals, with the ability to cause multiple organ damage in addition to affecting the cardiovascular system and predominantly the respiratory system. In addition, measures put in place to mitigate the pandemic such as self-isolation, travel restrictions, and social distancing can also result in adverse mental health effects.

The World Health Organization (WHO) has recommended several measures and policies to control the global spread of the virus that have been implemented locally to a varying extent. As different countries are at different phases of the outbreak, the policies and measures at a given time vary among different countries. However, the strategies used among different nations share several similarities. National policies and guidelines, which in some countries were enforced strictly for individuals, greatly helped to reduce the transmission of SARS-CoV-2.

Despite all efforts, this pandemic has been wreaking havoc across the globe, causing the number of infected patients to continue to rise. Fig. 1 shows the rate of infection (per 1000 population) and mortality rate (per 1000 infections) in different countries as of Apr. 17, 2021 [1], [2].

Most of the infected persons show mild symptoms. Therefore, they generally do not require hospitalization in many countries. However, they are required to self-isolate at home while keeping a cautious eye on the severity of the symptoms. Hospitalization rates increase with age [3], and rates of admission to intensive care units range from 5% to 22% depending on healthcare resources of different nations [4], [5]. As the disease progresses towards severe pneumonia, patients may start experiencing difficulties in breathing and lower oxygen saturation (SpO2) in blood due to alveolar damage, decreased lung compliance

© IEEE 2021. This article is free to access and download, along with rights for full text and data mining, re-use and analysis.

Authorized licensed use limited to: IEEE Xplore. Downloaded on October 07,2024 at 02:11:10 UTC from IEEE Xplore. Restrictions apply.

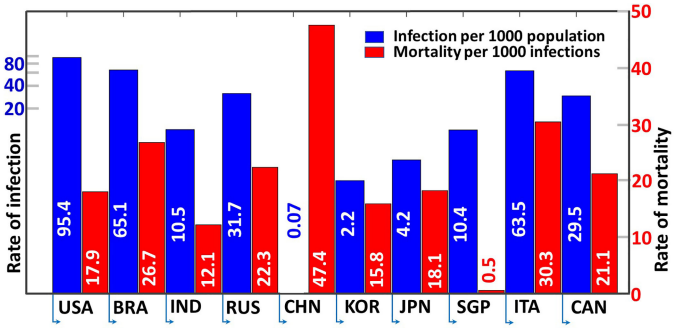


Fig. 1. Rate of infection (per 1000 population, presented in log scale) and mortality rate (per 1000 infections, presented in linear scale) in different countries as of 17 April 2021. ISO 3166-1 country codes are used to represent the countries.

TABLE I
COMMON SYMPTOMS IN COVID-19 CASES [6]

| Reported Frequency of Symptoms in COVID-19 Cases | |
|---|---|
| **Symptom** | **Percentage (%)** |
| **Fever** | 80.4 |
| **Cough** | 63.1 |
| **Fatigue** | 46 |
| **Expectoration** | 41.8 |
| **Anorexia** | 38.8 |
| **Chest tightness** | 35.7 |
| **Shortness of breath** | 35 |
| **Dyspnea** | 33.9 |
| **Muscle soreness** | 33 |

TABLE II
COMMON COMORBIDITIES IN COVID-19 CASES [7]

| Comorbidities in COVID-19 Cases | |
|---|---|
| **Comorbidities** | **Percentage (%)** |
| **Hypertension** | 60.1 |
| **Obesity (body mass index>30)** | 48.3 |
| **Diabetes mellitus** | 37.2 |
| **Pulmonary disease** | 22.3 |
| **Renal disease** | 13.7 |
| **Coronary artery disease** | 13.1 |
| **Asthma** | 11.3 |
| **Congestive heart failure** | 10.2 |

and reduction in the lung capacity. The common symptoms and comorbidities are shown in Table I [6] and Table II [7], respectively.

Therefore, considering the prevalence of Fever and Cough among the symptoms in the COVID-19 patients, it is critical to remotely monitor body temperature (BT) and cough, along with other important physiological parameters such as blood saturation oxygen level (SpO2), blood pressure (BP), heart rate (HR), heart rate variability (HRV), respiratory rate (RR), and lung capacity of COVID-19 patients in non-clinical settings to ensure efficient and effective utilization of healthcare service capacity. Ambulatory monitoring of COVID-19 symptoms in a continuous fashion allows for the early detection of severe and critical pneumonia, thus enabling timely medical intervention [8]. In addition, medical staff can use this wireless monitoring device in hospital settings to remotely monitor their patients as needed, thus reducing their frequency of visits to the patients' room and risk of infection, eventually leading towards effective and efficient use of the workforce and personal protective equipment.

Researchers in [8], [9],[10] provided the general outlook and recommendations for employing wearable sensor techniques for remote patient monitoring to cope with the outbreak of the COVID-19. In [10], the researchers showed that incorporation of wearable sensor data such from smartwatch and activity tracker on top of self-reported symptoms and diagnostic testing results can potentially lead to a superior model in identifying positive or negative COVID-19 patients among the symptomatic individuals. The results are however based on a relatively small sample of participants (8.7%) who were tested for COVID-19, disregarding a vast majority of (91.3%) of the participants who did not go for a COVID-19 test even after showing symptoms. Therefore, it is unclear whether this observation will still hold if this group of people would be included in the model. Nevertheless, this is an interesting work that further demonstrates the importance of wearable sensor-based monitoring of multiple bio-signals for a long period of time.

Most devices proposed in the literature do not feature an ergonomically comfortable and compact design for continuous monitoring of all aforementioned health parameters [8],[9],[10],[11]. Furthermore, most currently available commercial patient monitoring systems (such as from GE Healthcare, Philips Healthcare, Dräger, Welch Allyn, and Hexoskin) have limitations for the in-home monitoring of COVID-19 patients. In addition, these systems do not monitor coughing events, which is one of the most common symptoms among the COVID-19 patients and therefore critical to monitor [10],[11].

In this work, we present a brief discussion on the latest knowledge on the epidemiology of COVID-19, its impact on human health, and the measures adopted to prevent the spread of the coronavirus disease. We also present a review on some existing patient monitoring systems and propose a compact, wearable, smart system to remotely monitor vital-signs and important physiological parameters of the patients of COVID-19 or other chronic cardiorespiratory diseases. A software was developed to estimate BT, BP, HR, HRV, SpO2, RR, lung capacity, and cough using five types of sensors for – BT, electrocardiogram (ECG), photoplethysmography (PPG), sound, and motion. The algorithms were validated through experimental data obtained from lab volunteers and online databases including PhysioNET [12],[13] and Capnobase [14].

A brief overview on the current understanding of the health impacts of COVID-19 and adopted measures is discussed in section II. A review of the current state of the art of monitoring devices is presented in section III. The design of the system is described in section IV. The performance of the system was evaluated and discussed in section V. The perspectives and research challenges are presented in section VI. Finally, the research article is concluded in section VII.

## II. COVID-19: HEALTH IMPACTS AND POLICIES

### A. Epidemiology

Individuals who are symptomatic, pre-symptomatic or asymptomatic are all capable of transmitting the virus to other

Authorized licensed use limited to: IEEE Xplore. Downloaded on October 07,2024 at 02:11:10 UTC from IEEE Xplore. Restrictions apply.

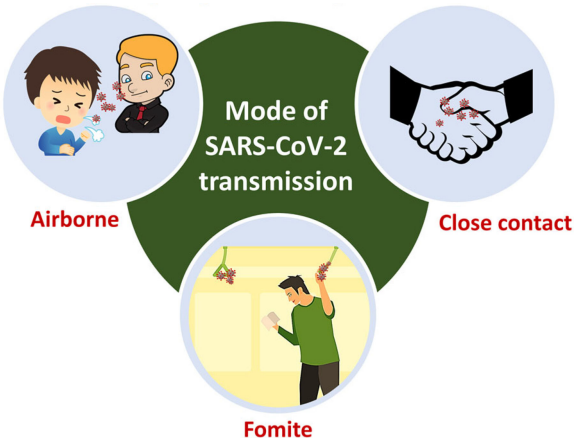


Fig. 2. Mode of transmission of SARS-CoV-2.

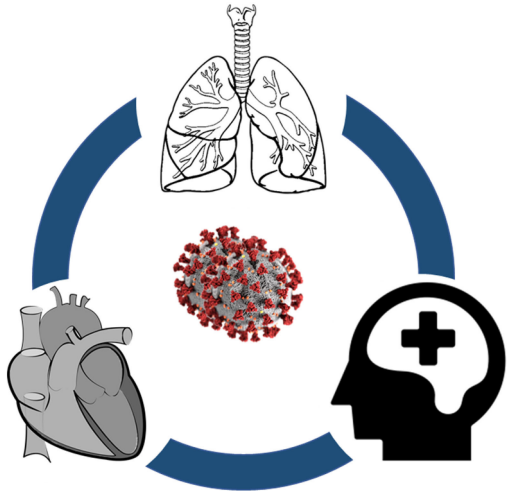

Fig. 3. Impacts of COVID-19 on human health.

individuals (Fig. 2). The virus is transmitted between individuals through contact with others and through respiratory droplets [15],[16]. These droplets may exist on surfaces on which an infected individual may have expired [17]. Droplets may also be propelled when interacting with others, such as when talking, coughing, or sneezing.

Once SARS-CoV-2 crosses a mucosal barrier, the receptor binding domain of the virus binds to human Angiotensin-Converting Enzyme 2 (hACE2), its receptor. Transmembrane protease serine 2 (TMPRSS2) then cleaves the virus to allow for membrane fusion [18]. The virus is also activated by furin and human proteases [19] and can induce changes in the host cell that may cause damage or kill the host cell, in addition to creating new viral proteins. New virus particles form at the Golgi body of the host cell, which are then able to reach the cell surface through vesicles for release and are able to infect subsequent cells [20].

Men are more likely to be infected and die from SARS-CoV-2 infection than women. Mortality rates and intensive care units (ICU) admission rates were also higher for males [21]. The severity of symptoms may also differ among infected individuals. 81% of symptomatic individuals suffer from mild to moderate symptoms, whereas 14% of symptomatic individuals experience severe symptoms and 5% of COVID-19 patients are in a critical condition [22]. 30.8% of infected individuals may also be asymptomatic [23]. Individuals with certain pre-existing medical conditions are also at an increased risk of experiencing more severe health effects as a result of infection. Examples of such conditions include kidney diseases, obesity, cardiovascular conditions, cancer, type 2 diabetes, and chronic obstructive pulmonary disease (COPD) [24]. Certain risk factors may also increase the likelihood of infection (such as age, race, poverty, crowding, medication use and pregnancy) [25]. The effective reproduction number can also provide information regarding disease spread among a population. In Canada, the effective reproduction number was at an average of 2.81 in mid-March 2020 but has decreased to 0.65 by mid-June [26]. The decreasing effective reproduction numbers seen in several countries, such as Canada and China [27] is promising, as a value below 1.0 indicates the slowing of the epidemic in those countries [28].

## B. Health Impacts

The SARS-CoV-2 infection causes several health problems to human body, predominantly affecting the respiratory system. Nevertheless, it can affect the cardiovascular system of the body. In addition, the measures and restrictions imposed on social interaction to control the transmission of the virus may cause mental health issues, and thereby affecting the overall health of an individual (Fig. 3).

***1) General Health:*** Once the virus reaches the alveolus, immune cells are recruited, and fluid accumulation occurs in the alveolus. The fluid in the alveolus alters the surface tension resulting in the start of alveolar collapse, causing breathing difficulties [29]. Although SARS-CoV-2 spreads mainly through the respiratory system, some individuals with COVID-19 also experience pathologies in multiple other organs [30]. This can be attributed to the cytokine storms, which was found to be the cause of death in 5% of critically ill patients due to multiple organ failure [31]. Organs which may be affected by an exaggerated immune response include the liver, kidneys, lungs and blood vessels [32].

Cardiovascular disorders were seen in COVID-19 patients with increased amounts of inflammatory biomarkers as well [5]. The nervous system is also affected in some patients, as demonstrated by the loss of the sense of smell, which is likely due to the virus reaching the brain from the epithelium of the nasal cavity [30]. At the cellular level, viruses may cause the death of a cell by inducing cell lysis or altering the cell's programmed cell death. However, it is also possible for the virus to use the host cell's machinery for replication without causing further damage to that cell [33]. Individuals with chronic illnesses are more susceptible to suffering from more severe adverse physical health effects upon infection. Particularly, individuals with respiratory diseases, cardiovascular diseases or diabetes are at an increased risk [34], in addition to those with compromised immune systems. Individuals in ageing populations are particularly at a heightened risk of suffering from more severe health conditions compared to their younger counterparts, as immunity

Authorized licensed use limited to: IEEE Xplore. Downloaded on October 07,2024 at 02:11:10 UTC from IEEE Xplore. Restrictions apply.

decreases with age [35] and older individuals are more likely to have other pre-existing health conditions.

***2) Cardiovascular Health:*** SARS-CoV-2, which was initially thought to be primarily a respiratory virus, has later been identified to inflict systemic disease. In particular, cardiac injury in COVID-19 patients is likely to be associated with overall higher morbidities and mortality as reported in [36].

The pathophysiology of cardiac changes is best characterized by overproduction of inflammatory cytokines (IL-1, IL-6), NK cells, and TNF-$\alpha$ cells leading to systemic inflammation and multiple organ dysfunction, acutely affecting the cardiovascular system. Furthermore, cardiac injury, defined as clinical, chemical (high troponin), or ECG changes, significantly relates to inflammatory biomarkers (Interleukins, C-reactive protein, BNP, Ferritin), suggesting an important correlation between myocardial injury and inflammatory hyperactivity triggered by a viral infection. Increased risk for myocardial ischemia or infarction, myopericarditis with depressed systolic left ventricle function, arrhythmias, thromboembolism, with sub-acute to long-term persistent myocardial changes that is suggestive of cardiomyopathies are described in patients with COVID-19 [37].

Children are much less infected (2-8% of all cases) so far with COVID-19, and when infected often having much less severe form of illness. However, a small number of children with Multisystemic inflammatory diseases of Childhood (MIS-C) were found to have signs of myocarditis, ischemia, and arrhythmia, however, showed rapid improvement in most cases with immediate intensive care management [38]. On the other side, persistent structural changes of heart and signs of inflammation were observed in COVID-19 patients with asymptomatic to mild symptoms, highlighting the long-term consequences of COVID-19 infection in setting the stage for cardiomyopathy and heart failure [39].

These cardiac involvements may be explained by the kinetics of cytokine storms. The natural arc of an immune response to an infection lasts for several days to weeks that ends to a resolution phase when the pathogen is controlled. For microorganisms with a high replicative potential, the rapid and widespread engagement of adaptive responses can lead to a rapid surge in immune activity associated with supra-physiological levels of circulating cytokines [40].

People with underlying cardiovascular problems such as high blood pressure, coronary artery disease, or heart failure were observed to be at a higher risk of infection and death. While the virus might directly inflict heart injury or Myocarditis in healthy people, things can get worse for COVID-19 patients with existing cardiovascular conditions because of increased stress and inflammation triggered by the body's overly aggressive immune response. Though Myocarditis often resolves without incident, it can lead to severe complications such as abnormal heart rhythms, chronic heart failure, and even sudden death. It was reported that as many as 7 percent of COVID-19 related deaths may result from myocarditis [41]. In addition, arrhythmia was very commonly observed among the COVID-19 patients [41]. Interestingly, viral proteins were identified in the heart muscle of six deceased patients, who however had neither any clinical signs of heart involvement, nor a prior history of cardiac disease and were documented to have died of lung failure [42]. The presence of SARS-CoV-2 in the heart muscle possibly explains COVID-19 induced cardiac damage [42].

Cardiologists estimate that half of the myocarditis cases resolve without a chronic complication [43]. However, several studies suggest that COVID-19 patients can show signs of myocarditis or myopericarditis months after contracting the virus [44]. Thankfully, some acute cases resolve on their own, requiring only hospital monitoring and possibly some heart medications. There are conflicting results of corticosteroids and intravenous immunoglobulin (IVIG) use in acute viral myocarditis in adults and older population [45]. There may be a role particularly for IVIG in younger patients who seem to present with more of a post- inflammatory multisystem inflammatory syndrome in children (MIS-C) type of the condition [46]. ECG is the most reliable method of detecting irregularities in the heart's rhythm and structure. A Holter monitor is generally used in the clinical settings as the portable means of recording a continuous ECG, usually for 24 to 72 hours, enabling detecting heart rhythm irregularities that cannot be observed during a regular ECG test [47],[48]. However, there are several FDA approved portable handheld single-lead ECG devices available in the market that can be used for long-term monitoring of the heart's activity at home. Other cardiac monitoring systems in the clinical settings include echocardiogram, computerized tomography (CT) scan, and magnetic resonance imaging (MRI) scan that can be useful for any structural and functional assessment of the heart. While cardiac assessment at rest is rich in medical information, Cardiopulmonary exercise testing (CPET) on cycle ergometry or a treadmill is an invaluable tool to assess functional exercise capacity, maximum VO2 consumption, the presence of cardiac ischemia during exertion.

***3) Respiratory Health:*** The most common acute respiratory illnesses are infections related to bacteria and viruses [49], [50] - SARS-CoV-2 being one of the deadliest types of the latter group. Respiratory infections can result in mild to moderate symptoms of fever, cough, and shortness of breath. This results in an inflammatory exudate in the airways with mucus production which can plug the airways [51],[52]. If this is not cleared by spontaneous coughing it can lead to a lobar collapse requiring more intense chest physiotherapy or suction with invasive bronchoscopy. When severity increases, an inflammatory exudate fills the alveolar air sacks (pus), leading to pneumonia. [53]. Pneumonia may progress to respiratory failure where oxygen levels in the arterial blood decreases and the CO2 levels in the arterial blood climb. This can be resolved by antimicrobial agents and death may be avoided. At this point of severity failure of other organ systems is sinister as the inflammatory responses can no longer be confined to the lungs. Mortality in such cases is high even with intensive care treatment with artificial ventilation, dialysis, circulatory support, ventricular assist devices, and extracorporeal gas exchange are required.

Numerous devices and techniques are available to assess respiration. The most commonly used tools to assess airways disease in the outpatient practice include the use of basic spirometry, which allows quantification of the forced expiratory volume in 1 second (FEV1), and the forced vital capacity (FVC), and

Authorized licensed use limited to: IEEE Xplore. Downloaded on October 07,2024 at 02:11:10 UTC from IEEE Xplore. Restrictions apply.

the inspiratory and expiratory flow rates. The FEV1 can be used to make a diagnosis of airflow obstruction (FEV1/FVC ratio $<$ 0.7, or FEV1/FVC $<$ lower limit of normal) and monitor disease progression. Some have proposed using impulse oscillometry to detect resistance in the airways [54]. More detailed pulmonary function assessments include assessment of total lung capacity (TLC), residual volume (RV), and functional residual capacity (FRC) in a body box. This is commonly supplemented with the assessment of the gas transfer capacity by measuring the diffusion/transfer of an inert gas (CO, Helium) across the alveolar membrane. This allows quantification of TLC involved in gas exchange, i.e., the communicating lung volume, the total lung diffusion capacity (DLCO), and the diffusion capacity adjusted for alveolar lung volume (KCO).

The most basic tools used in the inpatient practice involve monitoring of oxygen saturation using pulse oximetry, blood pressure, heart rate, and ECG. When assessing gas exchange, the arterial or capillary blood gas (ABG/CBG) quantifying the partial pressure of oxygen and carbon dioxide in the blood, along with pH and bicarbonate levels is performed. The assessment of the alveolar-arterial oxygen gradient measures gas exchange in the lungs. Ventilation/perfusion and diffusion varies widely in the acutely unwell patient. Basic imaging techniques such as the chest X-ray or high-resolution CT (HRCT) allow evaluation of the structure of the lungs and help clinicians make decisions about the need for a higher level of non-invasive or invasive ventilation. Failure of respiratory mechanics combined with the failure of gas exchange leads to respiratory muscle failure requiring ventilatory support devices. In such an acute ICU setting, if a patient is mechanically ventilated, assessment of the O2 consumption and CO2 production can be made on a breath-by-breath basis along with measures of airway resistance. An arterial line and a central venous catheter (CVC) line allow beat to beat accurate arterial and venous blood pressure. Extracorporeal membrane oxygenation (ECMO) is possible when all fails but this resource is expensive, scarce and addition of a substantial number of quality life years has not been convincingly demonstrated [55]. These monitoring tools and interventions are now routinely available in hospital settings to aid the management of acutely unwell patients.

With acute respiratory illness, people may develop symptoms of cough, shortness of breath, chest tightness, and wheeze. As the infection progresses, people may experience an abnormally higher heart rate, reduction in blood oxygenation, and an increase in the respiratory rate. However, some signs are often the later manifestations of the severity of respiratory illness. Therefore, there remains a need of detecting earlier changes in the respiratory function outside of the hospital setting.

Cough is a defining feature of many respiratory conditions including infections, asthma, COPD, and pulmonary fibrosis. However, there are only a few ambulatory cough monitoring devices that are FDA approved and CE/510K quality marked. One such device is VitaloJAK [56], which enables quantifying coughs objectively and is now the gold standard for clinical efficacy trials [57]. Nevertheless, these devices are not routinely available for clinical use and can record for only 24 hours. Therefore, cost-effective monitoring devices with longer recording capability are required [58], [59].

***4) Mental Health:*** In addition to affecting one's physical health, the COVID-19 pandemic may also affect the mental health of individuals. Common adverse mental effects include anxiety (being the most prevalent), depression and stress [60]. These adverse mental effects largely result from the precautionary measures taken to limit the spread of the novel coronavirus disease. The COVID-19 pandemic particularly affects the mental health of certain groups, such as health care workers, elderly individuals, those with pre-existing mental health conditions and those who are in social isolation or are homeless [60]. Healthcare workers are constantly exposed to COVID-19 patients and may have limited protective equipment, in addition to working extended shifts. They also must minimize social interactions with others and isolate themselves from family members, which are all factors that may compromise the mental health of workers and their families [60], [61], [62]. Individuals who must be in social isolation or confinement (for example, due to stay-at-home directives) are also at a heightened risk of experiencing adverse mental effects or disorders [62]. Individuals with pre-existing mental conditions, such as depression or anxiety, may face further difficulty adapting to a new lifestyle with reduced social interaction and uncertainty about the future [63]. Elderly individuals and those with pre-existing physical conditions (such as compromised immunity) may also experience increased emotional difficulty as they are more susceptible to experience the negative physical symptoms of COVID-19 and may have increased psychological distress surrounding their health [64].

It is crucial for regulations to be carefully implemented so as to reduce the spread of the virus while minimizing any adverse mental health effects to individuals. The strategic implementation of measures can ensure one's mental health and physical health are not extensively compromised.

### *C. Current Measures, Limitations and Recommendations*

Since human transmission of the virus is occurring at a rapid rate, several measures have been implemented by various levels of government around the world to decrease the transmission of the virus (Fig. 4). Globally, the World Health Organization (WHO) has recommended that all levels of government contribute to a response plan, reduce community transmission using physical distancing policies and implement travel restrictions as appropriate. The WHO also recommends for the coordination between different nations for an effective global response, in addition to suggesting the use of strategies which are adaptable [65]. Recommendations from the WHO and other governments continue to change as the pandemic evolves, as ongoing research further increases understanding of the virus and its transmission.

In the initial stages of the pandemic, China established fever clinics and recommended the use of face masks. In January 2020, the wearing of face masks in China was made mandatory, in addition to disinfection and handwashing being recommended,

Authorized licensed use limited to: IEEE Xplore. Downloaded on October 07,2024 at 02:11:10 UTC from IEEE Xplore. Restrictions apply.

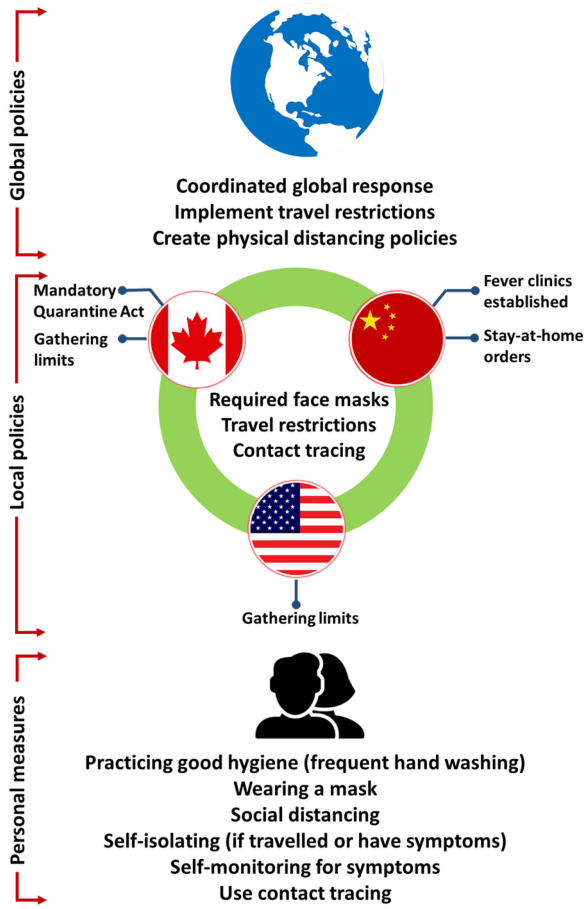


Fig. 4. Policies and measures adopted at different level to control the viral transmission.

after which a mandatory stay-at-home order was put in place [66].

In late January 2020, Canada began isolating individuals who were suspected of having COVID-19 due to travel, either in hospital or at home. Canada later began to implement travel restrictions, closing the U.S.-Canada border and reducing air travel, as well as implementing a mandatory Quarantine Act for individuals who arrive from other countries. Physical distancing, wearing masks and frequent hand washing were also recommended for individuals, and further restrictions such as gathering limits were put in place at the provincial level.

The United States federal government encouraged physical distancing and mask wearing, and travel restrictions were put in place. Decisions regarding restrictions in the United States, such as gathering limits, restaurant restrictions, stay at home orders and curfew, were largely made at the level of individual states [67]. The measures put in place at a given time may vary among different countries, as countries may be at different stages of the outbreak and thus implement differing mitigation strategies.

There is a great deal of similarity in the overall approach taken by different countries. For instance, several countries had shut down schools and businesses in an effort to reduce the spread of the virus, yet differed in the timing of the

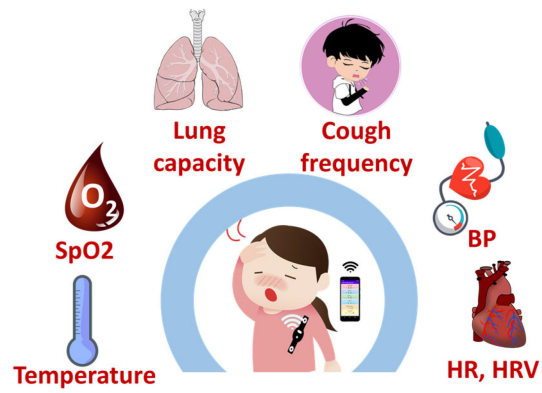


Fig. 5. Health parameters critical for monitoring COVID-19 patients.

implementation of policies. Furthermore, as different countries are at differing phases of the outbreak, it is difficult to plan for a coordinated global response. In addition, the use of tracing apps is beneficial for alerting individuals of possible contacts with infected individuals, but this also has some drawbacks, such as the lack of available technology in rural areas, not having all members of a population opting to use a tracing app, and privacy concerns. A potential recommendation to combat such drawbacks is to enforce stricter measures in areas where contact tracing is not used, or to mobilize technological resources to communities which are at a higher risk for community spread to benefit from such devices. Strong leadership at the international level to coordinate a global strategy with strict responsibilities for all nations can also help mitigate the pandemic and reduce the spread of SARS-CoV-2 at a much faster rate.

## III. RELEVANT MONITORING SYSTEMS

Unobtrusive monitoring of key physical signs is paramount for continuous ambulatory monitoring, particularly in the cases of self-isolation or self-quarantine [68],[69],[70]. As the wearable sensors are becoming progressively more comfortable and less obtrusive, they are an excellent choice for continuously monitoring an individual's health or wellness without interrupting their activities of daily living (ADLs) [71],[72],[73]. Therefore, it is no wonder that there is a growing trend among the researchers to develop wearable health monitoring systems to enable long-term monitoring at home [74],[75],[76],[77]. However, most devices reported in the literature do not support all the key parameters that are important for monitoring COVID-19 patients (Fig. 5).

### A. Non-Wearable Contactless Systems

***1) Wireless Systems:*** Researchers in [78] proposed a device to monitor breathing patterns and respiratory rate. They used an Impulse-Radio Ultra-Wideband (IR-UWB) radar-based technology to determine chest movements through the reflected waves, from which the respiratory parameters were extracted. The accuracy of the system was determined through the 6-min walk test (6MWT), where a subject walked in a straight path back and forth for 6 minutes. The respiratory signals received from

Authorized licensed use limited to: IEEE Xplore. Downloaded on October 07,2024 at 02:11:10 UTC from IEEE Xplore. Restrictions apply.

the complementary metal–oxide–semiconductor impulse radar chip were sent to an FPGA, where a Chirp-z transform block estimated the signal frequency, performed data compression and feature extraction. Based on the change in respiration intensity and change in I:E ratio before and after 6MWT, the authors reported achieving an accuracy of 73.3% in diagnosing respiratory diseases with the SVM in comparison to a spirometer. Through ANFIS, 68% FEV1/FVC index correlation was observed with a RMSE of 11.35. The proposed system can be used to screen for respiratory disease, such as COVID-19, through a completely contactless monitoring device. It also monitors this respiratory information continuously and passively without user input. The timing resolution and frequency are superior to previous design and processing the parameterized waveforms in the DSP backend is easy. The passive frontend architecture of the receiver features advantages of high linearity and low power consumption. Furthermore, it cannot extract cardiovascular information due to the high sensitivity required for detection of movements related to heart rate.

In [79], researchers used the channel state information (CSI) phase difference obtained using Wi-Fi signals to measure heart rate and respiratory rate by extracting the periodic signal induced by chest movements. The system consists of a commercial network interface card (NIC) and uses a smartphone/PC as the access point. A fast Fourier transform (FFT)-based method was used to detect heart rate, whereas the respiratory rate was estimated using a peak detection algorithm in the case of a single person, and a root-MUSIC (Multiple Signal Classification) method for multiple people. The system was tested in three different environments - a room crowded with tables and PCs, a through-wall scenario where the subject was separated from the receiver room, and a long corridor. The authors reported achieving a heart rate median error of 1 bpm, and a median error of 0.25 breaths per minute for the respiratory rate. This CSI-based method was reported to be highly robust for respiratory rate extracted at different distances and different orientations between the transmitter and receiver. In contrast to the UWB radar-based device reported in [78], this device has a lower cost, requires less bandwidth and no additional hardware, and can extract data from multiple people in a region albeit with a high error. However, the measured heart signal is much weaker than the breathing signal and thereby harder to detect properly as diastole and systole only cause small variations in the reflected signal. Furthermore, mean average errors (MAEs) increase while monitoring through wall and at long distance. Although both the devices reported in [78], and [79] are contactless, they only offer for monitoring a subset of vital-signs and restrict the users to stay within a limited range. In addition, the performance of these systems deteriorates sharply in the areas of high electromagnetic interference, especially in the case of detecting heart rate, thus making these solutions less feasible for continuous and ambulatory monitoring of COVID-19 7 patients.

***2) Phone-Based Monitoring Systems:*** Researchers in [80] have proposed a low-cost cell phone-based mobile pneumonia diagnosis method based on patient breathing sounds recorded using the phone. Recorded sounds were first normalized and down sampled from 44.1 kHz to 8 kHz, and each breath was manually annotated into seven different sub-segments of exhalation and inhalation. The authors extracted 18 acoustic features from the acoustic signal that included Prosodic, Spectral, Cepstral, Teager energy operator (TEO), and temporal information features. Finally, statistically significant features were fed into two ML classifiers, K-NN and SVM were used to classify pneumonia and non-pneumonia. The authors reported achieving pneumonia detection rates with a sensitivity, specificity, and accuracy of 92.06%, 90.68%, and 91.98%, respectively using the SVM classifier that are better or comparable to the diagnosis performance of a medical doctor or the existing contact-based methods. However, this method requires manual annotations of the breathing waveform, thus making it unsuitable for real-time application. In addition, accurate detection was only demonstrated for children ($<$5 years old) with results showing age-dependent coefficients, thus limiting the accuracy to this small age group who are not typically at high risk of COVID-19 infection. Furthermore, this method does not allow for monitoring cardiovascular or SpO2 data that are critical for COVID-19 patients.

Researchers in [81] proposed a method to detect respiratory infections using RGB-infrared sensors and a smartphone through monitoring the breathing pattern (such as I:E ratio), respiratory rate, and body temperature. There they attached a FLIR One Thermal Camera (RGB and Infrared) to an Android smartphone to obtain the thermal image sequence around the nostril. The sequence of thermal image was then analyzed based on a neural network proposed in Tang et al. [82] to identify normal or abnormal respiration condition. The authors reported achieving a sensitivity of 90.23%, specificity of 76.31%, and accuracy of 83.69%, in detecting respiration anomaly. A user-friendly smartphone application was developed to display temperature at the nose and head, processed signals, and the respiratory screening results. This contactless method of detecting respiratory anomaly allows for reliable screening through masks of varying sizes and thicknesses. However, the method cannot differentiate between different respiratory infections, as the screening results only display healthy vs. abnormal. In addition, breathing signals lose clarity outside of the 0.1 - 1.8 m range and a pitch rotation introduces error during measurement. Furthermore, this method does not allow for monitoring cardiovascular or SpO2 data that are critical for COVID-19 patients.

An AI-based speech processing framework was developed in [125] that exploits four biomarkers (muscular degradation, changes in vocal cords, changes in sentiment/mood, and changes in the lungs and respiratory tract) to pre-screen for COVID-19 from cough sound recorded with a smartphone. Cough recordings are transformed with Mel Frequency Cepstral Coefficient and fed into a Convolutional Neural Network (CNN) based platform that outputs a binary pre-screening diagnostic. The authors reported achieving a highly sensitive and specific pre-screening platform both for symptomatic and asymptomatic subjects that can potentially make it useful for daily screening at schools, workplace, and transport. Although the results are promising, the authors relied on the participants' personal assessment for diagnosing COVID-19 in more than half of the participants, thus potentially making the training data itself less trustworthy.

Authorized licensed use limited to: IEEE Xplore. Downloaded on October 07,2024 at 02:11:10 UTC from IEEE Xplore. Restrictions apply.

In addition, the authors did not cross-validate the model that further limits its reliability. Nevertheless, a rigorous clinical trial involving participants of different age groups and ethnicity is required to validate the efficacy of the model.

Researchers in [83] exploited AI techniques to diagnose COVID-19 with smartphones, through monitoring the frequency and intensity of cough. There they developed a smartphone application that records three spontaneous or nonspontaneous 3 second cough sounds at a sampling rate of 44.1 kHz using the built-in microphone of the phone. The audio sample was converted to the Mel-spectrogram, which was then fed into a CNN based classifier to determine a coughing event. Once the sound was identified as a coughing event, the data was then further passed through three different AI classifiers: Deep Transfer Learning-based Multi Class classifier (DTL-MC), Classical Machine Learning-based Multi Class classifier (CML-MC), and Deep Transfer Learning-based Binary Class classifier (DTL-BC). All three classifiers process and classify data independently that are later combined to obtain a conclusive COVID-19 diagnosis. The authors reported achieving a sensitivity, specificity, and accuracy of 96.01%, 95.01%, and 95.60%, respectively in determining if the input sound is a cough or not. The Deep Transfer Learning-based Binary Class (DTL-BC) classifier obtained a 94.57% sensitivity, 91.14% specificity, and 92.85% accuracy for COVID-19 detection. This simple mobile app-based solution proposition uses a simple mobile app to display real time results, making it completely contactless, and can be used by anyone in their own homes. Although the authors only relied on coughing events for COVID-19 diagnosis, it can be a potential preliminary tool for COVID-19 screening. However, a rigorous clinical trial is necessary to validate the efficacy of this screening app.

Researchers in [84], on the other hand, exploited a set of smartphone's built-in sensors, including the camera, microphone, and accelerometer and incorporated AI techniques to develop a smartphone-based COVID-19 monitor. The microphone was used to record coughing events, whereas the body temperature was extracted by analyzing the image captured by placing a finger on the smartphone's rear camera. The lung damage was assessed by analyzing the CT images scanned through the rear camera, and fatigue analysis was performed using the data from the accelerometer and camera based on the 30-sec sit-to-stand recordings. Breathing analysis was carried out by determining the inhalation and exhalation durations on the breathing waveform. All resultant data was fed to a 4-layer ML framework consisting of a recurrent neural network (RNN) and CNN for binary COVID-19 prediction based on symptoms levels. The CNN was used for abnormal CT-scan detection whereas other recorded data were fed to the RNN. The proposed system can potentially be useful as a contactless smartphone based COVID-19 detection tool both for the radiologists and general users. However, the authors did not report any experimental validation of their proposed technique, rendering its accuracy and reliability arguable.

Unlike the systems reported in [78] and [79], these phone-based systems require the users to participate actively to get their health parameters. In addition, the parameters can only be measured in short time frames, rather than passively monitoring them for a longer period of time. Furthermore, most of them do not offer monitoring cardiovascular data such as heart rate and blood pressure, and additional respiratory information including saturated blood oxygen levels that can be attributed to the restraints of a non-contact phone-based system.

### B. Non-Integrated Wearable Systems

An automated Arduino-based Multi-parameter monitoring system was proposed in [85] that was capable of monitoring blood pressure, heart rate, respiratory rate, and body temperature. The hardware consists of an Arduino Uno microcontroller interfaced with various sensors, including an airflow sensor, ECG sensor, pressure sensor, temperature sensor, and galvanic skin resistance (GSR) sensor. A Python program was developed and integrated with an eHealth platform that allows the patient to select the desired parameters to measure and visualize in real time. The proposed system is modular allowing new sensors to be added as required and comes with six different connectivity options such as Wi-Fi, 3G, GPRS, Bluetooth, 802.15.4, and ZigBee depending on the purpose. However, the components of the system are mounted inconveniently at various sites of the body including the arm, fingers, and face. In addition, some sensors require initial calibration for better accuracy, and software parameters may need to be adapted accordingly. Furthermore, the performance of the proposed system was not validated with any experimental data.

Researchers in [86] proposed a vital-signs monitor for the elderly that is capable of recording several different physiological signs including heart rate, blood pressure, $SpO_2$, and body temperature as well as making diagnostic decisions. The hardware consists of several commercial systems including a BP monitor, a finger-clip pulse oximeter, a tympanic thermometer, and a blood glucose meter. It also includes a set-top box which runs the software and transmits data to a computer. The central processing system processes the data and exploits an ANFIS-based artificial neural network to learn from the normal parameters of each patient where weightings were determined by consulting with physicians. The authors reported achieving excellent agreement with the physicians' diagnostic decision for tachycardia, hypertension, hypotension, hypoxemia, and hypothermia. The vital-sign data can further be sent to a tablet over the Bluetooth where data can be stored and displayed. The system was designed for seamless patient-doctor communication with real-time remote monitoring. Mapping and linking of multiple vital-signs for detecting a single event using fuzzy model AI yields high accuracy with reliable indication of health events. However, the system consists of isolated equipment, hence, is not portable or wearable. Besides, it does not provide measurements or estimations of respiratory rate and the cuff-based BP monitor is infeasible in the case of long-term monitoring. Furthermore, the dataset comes entirely from hospitalized elderly patients; therefore, potentially rendering the model biased towards that group of people and resulting a non-generalized model. In addition, further clinical investigations are required to test the proposed systems' in-depth capability in monitoring and diagnosing surgical patients and patients from the ICU.

Authorized licensed use limited to: IEEE Xplore. Downloaded on October 07,2024 at 02:11:10 UTC from IEEE Xplore. Restrictions apply.

A similar system was proposed in [87] for the elderly that is capable of recording blood pressure, heart rate, SpO2, and body temperature. The sensor system includes a pulse oximeter IC, two dry ECG electrodes, two reflective PPG sensors (DCM02), a temperature sensor, and a cuff-based BP monitor as the reference. The signals from the sensors are fed into a single handheld device. PPG and ECG peaks are detected through an adaptive peak detection algorithm, from where the pulse transit time (PTT) is calculated. HR is calculated from the ECG peak distances and SpO2 is calculated based on standard AC/DC calculation from two wavelength PPG sources. BP is estimated through standard pulse wave velocity (PWV) regression with least squares optimization using the reference device data. The authors reported achieving MAEs of 6.56 mmHg and 7.40 mmHg for systolic blood pressure (SBP), and diastolic blood pressure (DBP), respectively that is comparable to the results from other ECG/PPG monitors from the literature. However, the performance was evaluated only on two subjects. In addition, a cuff-based measurement of BP is required initially for subject-specific calibration. The device has split source, which in addition to the low noise power supplies allow both USB and onboard battery power. Nevertheless, the sensors are required to attach to the arm, fingers, and the ear, rendering the device not wearable or portable. In addition, inaccurate measurements are reported for heavy breathing (after exercise) or during motion. The dependency on HR for the BP estimation algorithm may potentially add extra noise to the estimation. The features of the portable patient monitoring systems are presented in Fig. 6

Fig. 6. Features of portable patient monitoring systems.

## C. Fully Integrated Wearable Systems

Researchers in [88] designed a headset that can measure various health parameters such as body temperature, frequency and intensity of cough, heart rate, and respiratory rate. There they housed several sensors that include in-ear headphones with built-in microphone, thermistor, and PPG sensor. The envelope detector of the mic signal is implemented using amplifiers and a Hilbert transform, converting the audio signal to a low frequency signal, reducing the frequency from 32 kHz to 25 Hz. The HR is determined from the FFT of the filtered PPG signal. RR was determined by performing FFT on the filtered microphone and Negative Temperature Coefficient (NTC) thermistor signals and identifying the dominant frequency. The user can position the built-in headphone mic inside a mask to improve portability in any environment. It is also possible to provide audio feedback through the headphones for alarms or alerts. In addition, the device requires low memory usage and is compatible with most smartphones. Although the extracted values were reported to be within a reasonable range, the quality of the measured signals and true accuracy of the estimations were not reported. The reliability of the acquired data may vary based on the headphones used and the quality if the built-in mic. In addition, spectrum analysis of long-term respiratory rate yields poor results.

A wrist-based smart watch named BioWatch was proposed in [89] that is capable of monitoring BP, heart rate, and $SpO_2$ as well as can improve BP accuracy by adapting to the individual and their postures. The device includes a PPG sensor, 3 dry electrodes for ECG measurement and a 9-axis MEMS inertial sensor and can be recharged through a micro-USB. PTT was derived from the PPG and ECG signals and BP was measured at rest for the first 4 minutes using a reference cuff-based BP monitor (CBM-7000) to obtain the normal PTT-BP correlation. The Valsalva maneuver that induces rapid change in BP was performed 5 times with a 45 second to 1-minute gap between each one and BP measurements were recorded using the BioWatch. A set of such measurements was obtained for each participant at three different postures such as standing, sitting, and supine. The device was tested using 5 different arm positions to determine which arm positions yielded the highest BP accuracy. During these trials, BP was estimated for 2-3 minutes. PWV was first estimated by PWV = d/PTT, where d = 50% subject height, as PWV has been shown to have a higher correlation to BP than PTT alone. Pulse pressure (PP), which is the difference between SBP and DBP (in mmHg), was determined through a regression using the PP values obtained from the reference BP wave, and their corresponding PWVs. SBP was calculated through a similar regression process, using reference SBP values and their PWVs from calibration. DBP was then calculated by subtracting PP from the SBP. The authors reported achieving root mean square errors (RMSEs) of 7.83-9.37 mmHg for SBP, and 5.77-6.90 mmHg for DBP. The use of PP estimations to calculate DBP resulted in higher accuracy than the conventional PTT-based approach that also eliminated the pre-ejection period

Authorized licensed use limited to: IEEE Xplore. Downloaded on October 07,2024 at 02:11:10 UTC from IEEE Xplore. Restrictions apply.

(PEP) errors generally included within the PTT. PEP is the delay between the QRS complex of the ECG and the actual blood ejection in the heart that introduces errors by adding delay to the PTT calculations, reducing accuracy of the BP-PTT relationship. However, the PPG waveforms obtained from the wrist have poor signal-to-noise ratio (SNR) in comparison to that from the fingertip, potentially leading to poor signals and estimation accuracy. In addition, changing arm position during training also may reduce the accuracy of results, and the arm also must be positioned close to the chest. The training algorithms use low complexity polynomial/exponential fits to save memory that may potentially limit the accuracy. Besides, the results presented are based on the fact that subjects performed the Valsalva maneuver that may not be generalized for other respiratory patterns. Furthermore, the SpO2 accuracies were not reported. Nevertheless, its ability of monitoring BP as well as for HR and SpO2 can be beneficial for COVID-19 monitoring provided that the system undergoes rigorous experimental validation.

Researchers in [90] also proposed a wrist-based system that is capable of extracting HR, HRV, and $SpO_2$ from a commercial wrist-worn pulse oximeter device (Wavelet Health sensor). The device includes used an Infrared and Red Reflectance PPG system (one red LED and one IR LED) that was worn on the right wrist. A smartwatch and commercial pulse oximeter were worn on the left arm for validation. PPG data was collected for ten minutes keeping the left hand at rest while moving the right hand in both periodic and random manner. The DC and AC components of the red and IR signals obtained from the raw PPG waveforms are separated using singular spectrum analysis (SSA) to obtain the ratio of light intensity, which SpO2 was finally calculated from. A high SNR red waveform was reconstructed by performing bivariate empirical mode decomposition (EMD) on the combined AC part of the infrared and red waveforms. Finally, Instantaneous HR was obtained by analyzing the PPG signals in frequency domain and the HRV was estimated by detecting the infrared PPG peaks. A mobile app was developed that can communicate with the device in real time over BLE and display recording prompts, battery percentage, and sync/desync. The authors reported achieving a MAE of 0.78 bpm, and 15.91 ms for HR and HRV (root mean square of successive differences (RMSSD)), respectively that are accurate and reasonable compared to the clinical/commercial devices. The SpO2 results from the last minute of the experiment achieved a MAE of 1.24% based on 5 subjects with respect to the PC68-B pulse oximeter as a reference. According to the author this is within the error of 3% present in similar commercial pulse oximeters. However, the estimation of SpO2 requires device calibration to improve accuracy and no comparison was made to the accuracy of the Wavelet Health sensor using its original algorithms. However, in comparison to the fingertip-based devices, PPG waveforms measured from the wrist generally suffer from poor SNR due to higher absorption and refraction of light, thus resulting in poor estimation of parameters.

Researchers in [91] proposed wearable cuff- and wrist-worn bands to monitor the mean arterial pressure, heart rate, heart rate variability, respiratory rate, and breathing patterns. The device consists of a cuff-based BP monitor with manual pump, Vernier pressure transducer, 2 thin conducting strips embedded in the inner sides of the bands. A BioHarness telemetry system was used for ECG data acquisition, composed of a data logger and USB Bluetooth device. The arterial pulse wave data was converted to analog voltage through the Vernier pressure transducer. The ECG R-peaks were identified using a previously reported QRS detector [92],[93] that was modified to augment its speed and accuracy. The arterial pulse peaks were detected by finding the maximum amplitude of each pulse peak between two R-peaks, and corresponding R-R interval and pulse to pulse (PP) interval were derived. Respiratory patterns were extracted from the arterial pulse waves and ECG data based on amplitude and frequency modulation methods. These methods included analyzing ECG amplitudes, ECG intervals, pulse wave amplitudes, and pulse wave intervals. The authors reported to achieve an MAPE of $\sim$0.94% for their respiratory rate measurements and nearly 100% agreement between the ECG-derived and pulse wave derived HR. This device used conducting fabric instead of dry ECG electrodes that reduces hardware complexity and improves wearability and comfortability for long term use, while preserving accuracy. In addition, the device is capable of monitoring a wide variety of parameters including cardiovascular and respiratory related signs. However, the arterial pulse wave signals at pressures below and between 30-40 mmHg yield unsatisfactory results. Furthermore, the SBP and DBP measurements were not reported. The experiments were conducted on a small group consisting of only six healthy subjects. More experiments from a diverse group of subjects are required for a better assessment of the device. Although real time transmission of the raw data (ECG and arterial pulse wave) seems possible, the device, however, offers no real time data transmission that may potentially limit its long-term usage.

Researchers in [94] extracted respiratory information from the oscillometric BP waveform obtained from a traditional cuff-based BP device and used it further to blood pressure, heart rate, and respiratory rate. The oscillometric method is the most common BP measuring method that exploits the pressure variations in the BP cuff caused by the oscillation of blood flow to determine SBP, DBP and mean arterial pressure (MAP). The hardware consists of just a wearable cuff-based BP monitor. The data collection procedure involves 6 consecutive left-arm BP measurements, with 3 measurements at rest, followed by 3 measurements while squeezing a ball with the right hand. This is preceded and followed by BP measurement using the clinically validated device. The SBP and DBP values were estimated from the pressure and oscillometric waveforms using the traditional oscillometric method. HR was calculated from the frequency spectrum generated via the FFT of the oscillation waveform, in which the frequency component with the highest magnitude corresponds to the heart rate. The authors reported achieving high performance with a MAE of 3.57 mmHg for SBP, 2.45 mmHg for DBP, 0.75 bpm for HR, and 2.69 breaths per minute for RR from a group of 40 subjects. This method does not need any additional calibration and improves upon traditional automated respiratory rate measuring techniques which often interfere with the ability for normal breathing. In addition, the system's capability of monitoring vital-signs associated with

Authorized licensed use limited to: IEEE Xplore. Downloaded on October 07,2024 at 02:11:10 UTC from IEEE Xplore. Restrictions apply.

both the heart and lungs makes it a promising tool to monitor respiratory infectious diseases such as COVID-19. It can estimate respiratory rate to a better or similar degree than from ECG/PPG signals during rest. However, the respiratory data from traditional ECG systems has been shown to have a higher accuracy for long term measurements.

Researchers in [95], [96] developed a wearable chest patch that can record heart rate, HRV and respiratory rate. It can also monitor activities such as step count, walking/running, and postures. The hardware consists of two parts: the wearable adhesive patch, and the reusable electronics module (REM). The adhesive patch contains single-lead, bipolar hydrogel disc covered ECG electrodes. The REM contains an embedded processor, a tri-axial accelerometer, and a BLE transceiver. The device was evaluated at different conditions that included sitting breathing exercises, ADLs, stationary cycling, simulated falls, and various postures. HR and respiratory rate were obtained by identifying the peaks in the ECG and respiratory signals, respectively. A linear correction was applied to each respiration rate to correct for proportional biases, and the final respiratory rate is calculated as the weighted mean between individual respiratory rates. The authors reported achieving a respiratory rate MAE of 1.1 breaths per minute, heart rate MAE of $<2$ bpm, and HRV RMSSD of $<15$ ms. In addition, step detection had a mean average percent error (MAPE) of 3.5%, and posture detection median had 96.3% accuracy. This device exploits the accelerometer to compensate for motion artifacts in the ECG and breathing data thus making the signals less sensitive to movement. The use of a computationally efficient approaches for respiratory rate detection makes it suitable for low-power device. In addition, this proposition exploited a weighted approach across components resulting in good improvements over traditional approaches. It features sensor fusion between the ECG and tri-axial accelerometer by combining respiratory signals and using a final respiratory rate which resembles the most accurate signals only. However, adequate electrode to skin contact is required for ECG data, which may require cleaning and shaving of the attachment location on the chest. Besides, chest movements can corrupt the accelerometer data during ADL measurements. In the case of RSA (respiratory sinus arrhythmia), the ECG was found to miss half of the measurements.

Researchers in [97] also proposed a chest-mounted device that can monitor blood pressure and heart rate. There they estimated BP by incorporating the seismocardiogram (SCG) waveform obtained from the accelerometer to estimate PTT without including the PEP. The device includes PPG sensor with 850nm IR LED and 2 photodiodes, accelerometer, and 2-lead ECG. A cuff-based reference BP monitor was used for a short period of time to obtain the subject-specific coefficients. PPG and SCG signals between two consecutive R-peaks were segmented and all such segments within a period of 10 seconds were averaged, resulting in one PPG and SCG in a single cardiac beat in 10 seconds. The SCG max peak, which is associated with the aortic valve opening (AO) is determined, then the maximum valley prior to AO was determined as the SCG amplitude (SA). The intersecting tangent (IT) point was detected on the PPG, and PTT is calculated as the AO-PPG IT distance. Finally, BP was estimated through a calibrated regression model that is proportional to log (PTT) and linear with SA, using reference BP values from the cuff-based monitor. The authors reported achieving mean absolute deviations (MADs) of 4.05 mmHg and 2.50 mmHg for SBP and DBP, respectively from the short-term trails. However, MADs of 9.41 mmHg and 8.44 mmHg for SBP and DBP, respectively were observed during the daily monitoring period. This device outperforms many conventional PTT-based and PAT-based BP estimation devices in short-term BP monitoring. However, the quality of the PPG waveforms obtained from the chest surface is poor, due to the lack of blood perfusion compared to the finger, toe, or ear. The adoption of low power design techniques made it suitable for continuous monitoring for a long-term period, although the estimation noticeably loses accuracy in long-term monitoring.

Although it is encouraging to see many researchers and companies around the globe working to develop portable, affordable and long-term tools for health monitoring, most of them are however limited by their monitoring time and capability of monitoring a few physiological parameters. In addition, most reported monitoring systems require active participation of the users and restrict their physical independence. Another concern about the wearable systems evolves from their ease-of-use [68], [126] particularly among the older population who reportedly showed a tendency of not even activating their wrist-based fitness devices [126]. Therefore, a wearable system must be user-friendly in terms of initial setup, connectivity and operational procedures. Also, an easier initial set-up process can encourage the users to continue using the devices [68], [126].

Nevertheless, all these promising research works on portable and affordable monitoring tools can potentially pave the way towards realizing a compact and wearable health monitoring system. However, rigorous clinical trial, which most of them currently lack, must be conducted to validate the clinical efficacy of these tools. Fig. 6 presents the summary of the portable patient monitoring systems discussed in this section.

## IV. PROPOSED MONITORING DEVICE

### A. System Specifications

As discussed in section I, the most common symptoms of COVID-19 include fever, shortness of breath and dry cough. Some individuals may also show the elevated blood pressure, increased heart rate, loss of taste and/or smell, and diarrhea. As the disease progresses towards severe pneumonia, the patient may start having difficulty in breathing, which is likely due to reduced lung function/capacity. Consequently, the oxygen level in the blood may reduce to below the normal range.

Health condition may deteriorate rapidly in some patients that may require immediate medical attention in the form of ventilation and admission to the ICU. Therefore, it is critical to remotely identify and monitor these symptoms in non-clinical settings to ensure efficient and effective utilization of healthcare service capacity. To deal with this, we propose a wearable tele-health monitoring system, which allows for the identification of critical patients early enough for timely medical intervention.

Authorized licensed use limited to: IEEE Xplore. Downloaded on October 07,2024 at 02:11:10 UTC from IEEE Xplore. Restrictions apply.

TABLE III
MONITORED PARAMETERS, USED SENSORS, SPECIFICATIONS, AND MEASUREMENT APPROACH

| Parameter | Sensors | Specification | Measurement type |
|---|---|---|---|
| Body temperature | Temperature sensor | ± 0.1°C | Direct measurement |
| HR and HRV | Dry electrodes | ± 1% or ± 2 bpm | Derived from ECG |
| SpO2 | Photodetector | ± 2% | Derived from PPG signal |
| Cough | Microphone, accelerometer | | Sensor fusion |
| Respiratory rate | ECG, accelerometer | ±1 breath/min or ± 2% | Sensor fusion |
| Blood pressure | Dry electrodes, photodetector | SBP:3.41 ± 2.17, DBP:1.61 ± 1.49 | Derived from ECG and PPG signals |
| Lung function | Microphone, accelerometer, photodetector | FEV1 & TV* | Sensor fusion and AI |

(*FEV1 – forced expiratory volume in 1 second and TV – tidal volume (Future work)).

On the patient side, a multi-sensor data acquisition module containing five types of sensors for – temperature, ECG, PPG, sound (microphone) and motion (accelerometer) is used to measured BT, HR, HRV, SpO2, coughing, BP, RR. The lung function/capacity can further be estimated by exploiting sensor fusion techniques. The data from multiple sensors are sent over Bluetooth to a local node that performs data alignment and initial signal processing. The pre-processed data from the patient side are then sent to the central server for further processing such as data archiving, fusion, detailed analysis and visualization. Finally, the physiological data can be viewed by the health provider on the terminals such as cellphones, tablets or computers. The multi-parameter monitoring capability of the proposed system can also be used to monitor patients with chronic cardiorespiratory diseases.

The specifications of the proposed system were determined by analyzing the requirements for monitoring COVID-19 patients and comparing other patient monitoring systems from the literature and available commercially. The specifications ensure precise and reliable monitoring of the patients' physiological condition. The sensors used in the proposed monitoring system, their specifications and the parameter measurement/estimation methods are summarized in Table. III.

## B. Hardware Design

We investigated and compared the performance parameters of the required sensors to achieve the system specifications. The following sensors are selected to obtain the required physical parameters in the wearable monitoring system.

***1) Sensor Selection:*** *Temperature sensor:* Temperature sensor measures body temperature. The low-cost NTC (negative thermal coefficient) thermistors or silicon-based sensors (< $1) are commonly used for the temperature measurement of the contactable surface. Here, a silicon-based sensor (LMT70YFQT) is chosen in our proposed system. The typical accuracy is ±0.05 °C from 20 °C to 42 °C [98]. The sensor is embedded in an elastic band and mounted on the chest to ensure good contact with the skin, which guarantees an accurate body temperature measurement.

*ECG and PPG Sensor:* There are two types of PPG sensors: transmission type and reflection type. Since the proposed monitoring device is mounted on the left chest, we choose a reflection-type PPG sensor. This PPG sensor works by shining the red and near IR light to the artery. The reflective optical power is then collected by the sensor to determine the SpO2 from the difference of the light absorption by oxyhemoglobin (HbO2) and hemoglobin (Hb) at the red and near IR wavelengths, respectively.

The ECG sensor is used to provide the standard single-lead ECG waveforms, from which the physical parameters such as RR, HR, and HRV can be retrieved. The ECG signal can also be fused with PPG signal to estimate the BP and to improve the accuracy of other parameters such as RR, HR, HRV. The ECG and PPG signals need to be time-synchronized to obtain an accurate estimate of BP. Therefore, an integrated ECG and PPG sensor MAX86150 is chosen for the proposed system [99]. This sensor consists of a photodetector, red/IR LEDs and low-noise readout electronics for the single-lead ECG sensor module and can provide synchronized ECG and PPG (both red and IR wavelength) signals.

*Microphone:* A microphone is used to record the sound of cough. The acoustic properties of cough sounds are analyzed to estimate several important parameters such as cough frequency, intensity and patterns. An omnidirectional electret condenser microphone (CMC-6027-24L100) is chosen for the cough monitoring module due to its high sensitivity, which is typically -24 dB when measured with a 1 kHz sine wave at a 94 dB sound pressure level (SPL) [100].

*Accelerometer:* The accelerometer does not directly generate a physiological parameter. However, the output signal from the accelerometer can be used to estimate the degree of chest expansion such as respiration, coughing events. This information, in addition to the information from the ECG, PPG and microphone will be used in an AI-based platform to achieve a surrogate measure of lung function. In addition, the accelerometer data can also be used to estimate and correct for motion artifacts in the ECG and PPG signals. A small, low-power and highly integrated inertial measurement unit (IMU) BMI160 is used in the monitoring system. The IMU includes a tri-axial accelerometer, which quantifies the chest movement. The complete patient monitoring system is shown in Fig. 7.

***2) Fast Prototype:*** To evaluate the feasibility and performance of the proposed monitoring system, a fast prototype was built by integrating the aforementioned sensors, off-the-shelf evaluation boards and data acquisition device. A MAX86150 Evaluation System comprising a sensor board (MAX86150 evaluation kit) and a data acquisition and transmission board (a MAX32630FTHR microcontroller board) is used to get the synchronized ECG and PPG signals [101]. The MAX86150 evaluation kit was modified to enable a flat surface on the board that allowed for mounting the monitoring system on the left chest.

Authorized licensed use limited to: IEEE Xplore. Downloaded on October 07,2024 at 02:11:10 UTC from IEEE Xplore. Restrictions apply.

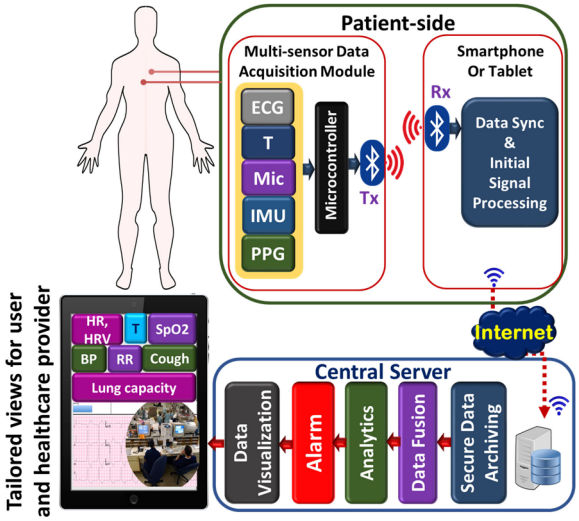


Fig. 7. Complete patient monitoring system.

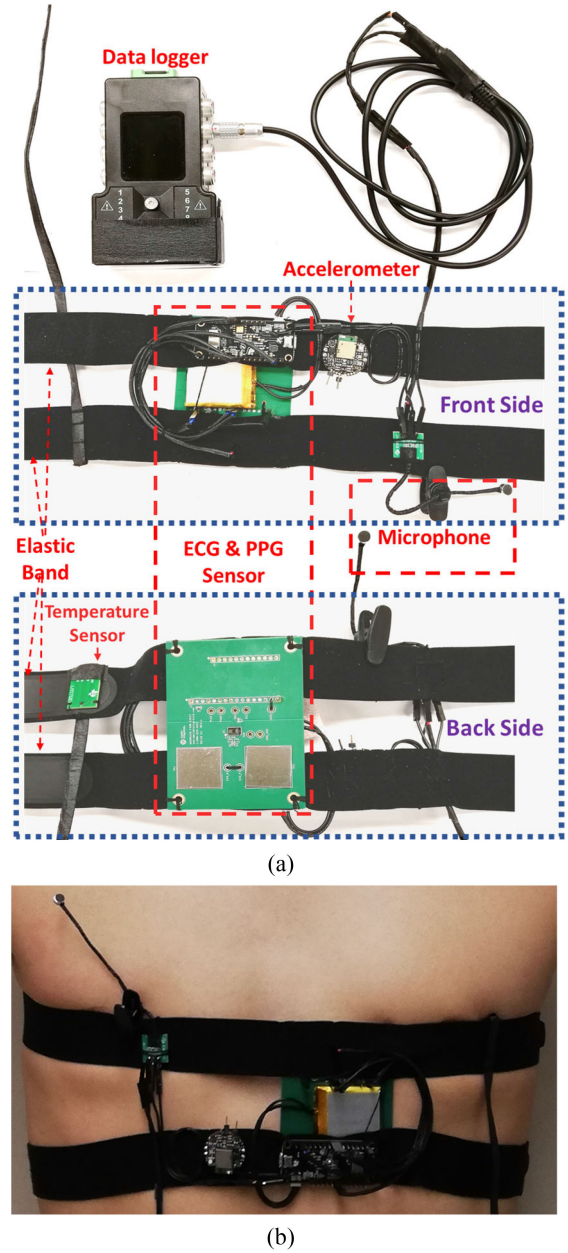


Fig. 8. Wearable health monitoring system a) hardware prototype b) mounting on the chest.

For the cough monitoring module, a data logger (Biometrics DataLOG MWX8) was used to acquire the analog output signal from the electret condenser microphone (CMC-6027-24 L 100) [102]. The data logger has a reconfigurable input signal range and sampling rate and can store the recorded data into the local SD card and/or send to a computer through Bluetooth. The accelerometer signals are obtained from an IMU board (MetaWear CPro) [103], which transmits data wirelessly into a smart device for further processing. A LMT70 temperature sensor evaluation module (LMT70EVM) [104] was used to measure the body temperature. The prototype of the monitoring system and its mounting on the chest are presented in Fig. 8.

## C. Computing Platform Design

The software methods used for processing the acquired signals are implemented in MATLAB and include the signal processing of raw PPG and ECG signals collected by the proposed device. These two signals can be processed to output parameters including HR, HRV, SpO2, RR, and BP. The overview of the computing platform is presented in Fig. 9.

***1) Signal Processing:*** The raw PPG signals (both infrared and red wavelengths) go through a filtering process which includes a 10th order polynomial detrend and a 4th order bandpass Butterworth filter with cutoff frequencies of 0.5 and 5 Hz. The infrared light PPG signal was found to have better SNR compared to the red light PPG signal in general, and therefore was chosen for feature extraction, which includes finding the maxima and minima of the signal that correspond to the systolic peak and endpoints of the pulses, respectively.

The period of the PPG pulses is estimated by identifying the dominant frequency through FFT analysis. Outlier data resulting from motion or noise artifacts are first removed. Then, a threshold of 0.4 times the maximum PPG value is used with MATLAB's findpeaks function along with the wave period to detect PPG pulse maxima and minima. Any abnormally large peak interval windows are continually rescanned with an adjusted threshold local to each window to find any missing points of interest.

The raw time-synchronized ECG data is detrended and passes through a bandpass filter with cutoffs at 8 and 40 Hz. ECG R-peak detection uses a similar threshold-based approach, with 0.6 times the average maximum value being the minimum acceptable R-peak value. Points where the time intervals between the ECG and corresponding PPG peaks are abnormally high or the ECG signals experience motion or noise artifacts are eliminated.

***2) HR and HRV:*** HR and HRV are determined based on R-peak spacing in the time domain, i.e., the R-R intervals.

Authorized licensed use limited to: IEEE Xplore. Downloaded on October 07,2024 at 02:11:10 UTC from IEEE Xplore. Restrictions apply.

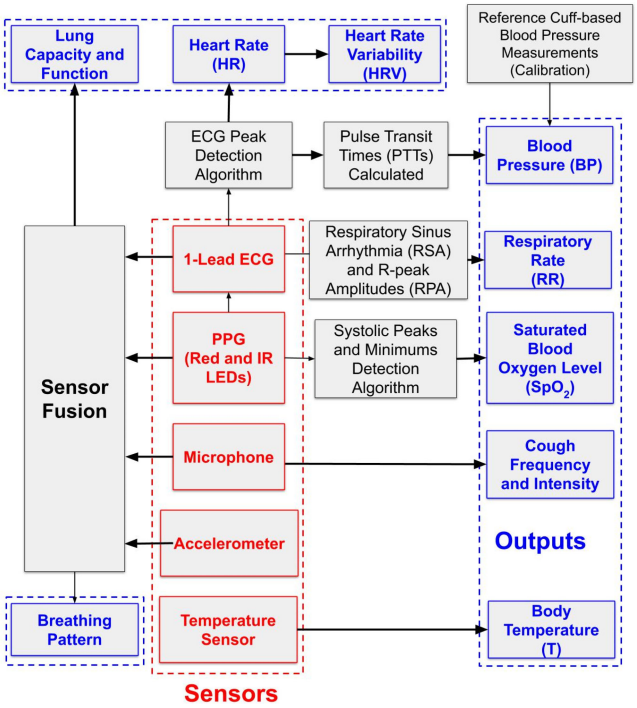


Fig. 9. Overview of the computing platform.

Upper and lower limits are determined based on the median RR-interval. The R-R intervals outside of this range are discarded. Heart rate is determined as the inverse of the mean accepted R-R interval, converted to beats per minute. HRV is calculated in the time-domain as the RMSSD of acceptable R-R intervals [68].

***3) SpO2 Estimation:*** SpO2 can be obtained from the red and infrared (IR) PPG signals using Eq. 1[105].

$$SpO2\ (\%) = 110 - 25 \times R. \tag{1}$$

Here,

$$R = \frac{RMS_{ac(red)}}{DC_{red}} \Big/ \frac{RMS_{ac(IR)}}{DC_{IR}}. \tag{2}$$

The AC component of the PPG signals corresponds to the pulsatile part of arterial blood volume, while the DC component represents the non-pulsatile part. The oxygenated hemoglobin in the blood absorbs IR and red wavelengths of light differently [106],[68]. Highly oxygenated blood absorbs more IR light than the red light, resulting in a larger IR signal than the red signal and consequently a smaller *R* and higher *SpO2*. Conversely, at lower oxygenation, the relative absorbance of the red wavelength is higher than the IR light, resulting in a higher *R* value, and lower *SpO2*.

However, instead of using the root mean square or mean values of the entire PPG signals as shown in [105], the AC and DC values are calculated for each PPG pulse. This allows for detecting and discarding the outliers in the estimation and makes the estimation of SpO2 more accurate and robust against noise and motion artifacts.

***4) PTT and BP:*** PTT is the delay for the pulse pressure wave, reflected as the dilation of the arterial wall, to travel from one arterial site to another [107]. PTT is known to have a strong negative correlation with systolic blood pressure (SBP), whereas PTT and diastolic blood pressure (DBP) have a relatively weaker, but observable inverse relationship [108].

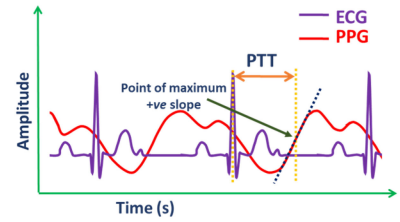


Fig. 10. Typical representation of pulse transit time (PTT).

PTTs are calculated as the time difference between each validated ECG R-peak and the point on the neighboring PPG rising portion with the highest slope (Fig. 10). Past research has suggested using one of many PPG feature points such as the peak, minimum, or the point with a maximum positive slope in PTT calculations. However, using the point with maximum positive slope was found to provide the most reliable results. The PWV can be estimated using the Moens–Korteweg equation using parameters including PTT and the distance of the sensor from heart ($L$) [109].

Here, PWV is expressed in terms of the elastic modulus of the artery wall ($E_{in}$), the arterial wall thickness ($h$), the density of blood ($\rho$), and the artery radius at the end of diastole ($r$).

$$PWV = \frac{L}{PTT} = \sqrt{\frac{E_{in}\, h}{2\, \rho\, r}} \tag{3}$$

The arterial wall elastic modulus can be expressed as a function of mean blood pressure, $P_t$ as demonstrated in [110],

$$E_{in} = E_0\, e^{\gamma\, P_t} \tag{4}$$

where $E_0$ and $\gamma$ are constant coefficients. The values of these coefficients are the same used in [111], found through an experimental fit, where $E_0 = 1429$ mmHg and $\gamma = 0.031$ mmHg$^{-1}$. Using both equations, a one-point calibration model was constructed, as in [111].

$$DBP = \frac{1}{3}\, SBP_0 + \frac{2}{3} DBP_0 + \frac{2}{\gamma} \ln\left(\frac{PTT_0}{PTT}\right) - \frac{(SBP_0 - DBP_0)}{3}\left(\frac{PTT_0}{PTT}\right)^2 \tag{5}$$

$$SBP = DBP + (SBP_0 - DBP_0)\left(\frac{PTT_0}{PTT}\right)^2 \tag{6}$$

One reference BP pair ($SBP_0$ and $DBP_0$) is obtained from a cuff-based BP monitor and its corresponding $PTT_0$ are together used for cuffless estimation of BP for the rest of the time interval.

***5) Respiratory Rate:*** The ECG waveform also contains information about the respiratory sinus arrhythmia (RSA) and the modulation of R-peak amplitudes (RPA). RSA represents the changes in heart rate due to respiration, in which the ECG R-R intervals are shortened during inspiration and prolonged during

Authorized licensed use limited to: IEEE Xplore. Downloaded on October 07,2024 at 02:11:10 UTC from IEEE Xplore. Restrictions apply.

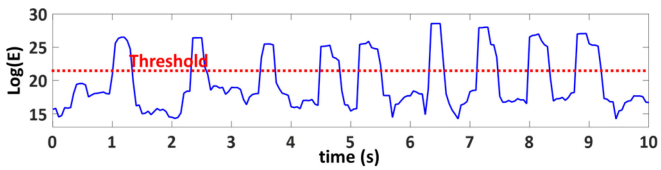


Fig. 11. Cough signal energy with time.

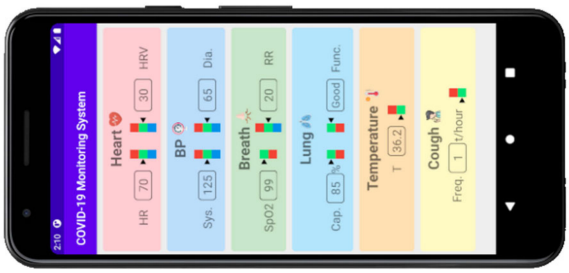


Fig. 12. Graphical user interface (GUI) application demo for the display of physical parameters from the wearable monitoring system.

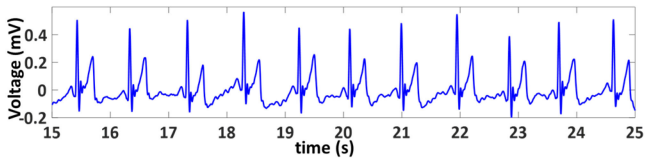


Fig. 13. A sample ECG measured with the proposed system.

expiration [112]. Respiratory rate can be estimated solely from the PPG or ECG RSA; however, estimation accuracy can be improved by fusing information from both the RSA and RPA waveforms. The RSA and RPA waves are extracted following the procedure reported in [113] and are fused to estimate the RR.

Firstly, for RSA extraction, a new vector is created which stores R-R intervals (in ms), where each index corresponds to the time that the interval occurred. The time of occurrence is chosen as the midpoint between each ECG R-peak for each R-R interval. Cubic spline interpolation is used to resample this new vector data at 2 Hz, acquiring the interbeat interval waveform (IIW). Finally, the RSA waveform is acquired from the IIW using a 6th order Chebyshev type 1 bandpass filter, with cutoff frequencies between 0.1 and 0.5 Hz, and a 3 dB passband ripple, employed forwards and backwards. The same filtering process is used for the RPA wave, however, instead of the R-R interval, each point in the new vector represents the R-peak amplitude at that time. Both time-domain and frequency-domain analysis are performed on the RPA and RSA waveforms. In the time-domain, peaks of the breathing pulse are identified, where peaks must be at least 1 second apart such that the breathing rate is <60 breaths per min. The inverse of the mean breathing interval is then used as a candidate for breathing rate. In the frequency-domain, FFT dominant frequencies are found for the RSA and RPA waves. If they are found to be too noisy, the time-domain analysis candidates are used alone. Otherwise, a common dominant frequency is found between the RSA and RPA and chosen as the breathing rate once converted to breaths per minute.

***6) Cough Frequency:*** The microphone signal was first filtered by a low-pass Butterworth filter with a cut-off frequency of 250 Hz. The signal was then segmented into 0.2 s windows with an overlap of 0.05 ms. The natural logarithm of signal energy ($E$) for each window was calculated. Finally, a threshold was applied on the signal energy to detect a cough (Fig. 11). The cough frequency then can be obtained by counting the total number of coughs in an hour.

***7) Lung Volume:*** The motion data from the chest-mounted accelerometer was used to estimate the lung volume. The chest expands with inhalation and the more air is inhaled, the more expansion the chest experiences. Therefore, the accelerometer can be reliably used as surrogate tool for estimating lung volume. In a preliminary attempt to estimate the lung volume from the accelerometer data, it was first filtered using a fourth-order low-pass filter with a cut-off frequency of 1 Hz. The spectral density of the signal was then calculated by using FFT. The spectral density of the accelerometer signal corresponds to the amount of air inhaled by the lung.

### D. Graphical User Interface for Data Visualization

An Android-based graphical user interface (GUI) application was designed to display the physical parameters measured using the proposed wearable monitoring system, as shown in Fig. 12.

The physical parameters were divided into 6 categories: Heart (HR and HRV), Blood pressure (SBP and DBP), Breath (SpO2 and RR), Lung (capacity and function), Temperature (T) and Cough (Frequency). A color bar was designed for each parameter to indicate whether the parameter is in the normal range. The green color means the parameter is in the normal range while the red color indicates the parameter exceeds the normal range and the blue color denotes the parameter is below the normal range. These indicators provide an easy way for the users to assess their health condition.

## V. PERFORMANCE EVALUATION

### A. Hardware Validation

The proposed monitoring system comprises several sensors and peripheral circuitries. Therefore, it is necessary to validate the function of the integrated device to ensure that it meets the specifications consistently and reliably.

***1) ECG Signal:*** The ECG signals were acquired from the chest. A sample ECG signal is shown in Fig. 13. The characteristic peaks of the ECG signals i.e., P, QRS complex and T waves are readily identifiable in the measured signal.

***2) PPG Signal:*** The MAX86150 Evaluation system can provide reflective PPG signals with red and IR wavelength lights emitted from the built-in LEDs. The red and IR PPG signals measured from fingertips and left chest are shown in Fig. 14.

Since the commercial pulse oximeter usually show a calculated value rather than the raw PPG waveforms, it is difficult

Authorized licensed use limited to: IEEE Xplore. Downloaded on October 07,2024 at 02:11:10 UTC from IEEE Xplore. Restrictions apply.

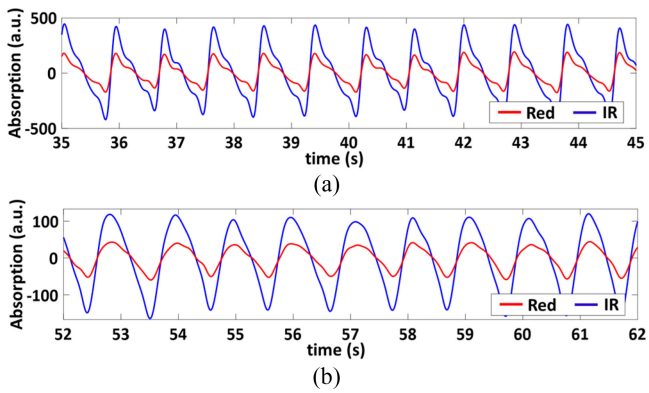


Fig. 14. Measured PPG signals from a) fingertip, and b) chest.

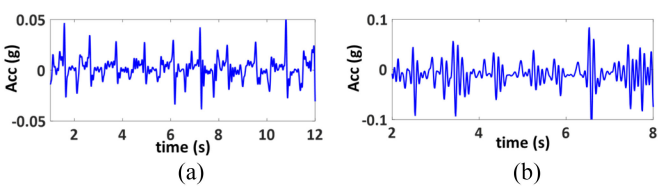


Fig. 15. Chest movement measured with accelerometer a) respiratory expansions b) coughing.

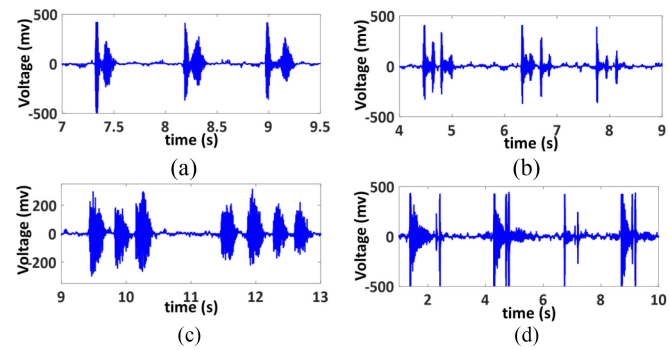


Fig. 16. Acoustic signals of different coughing types a) single cough b) double cough c) throat clear, and d) wheezy cough.

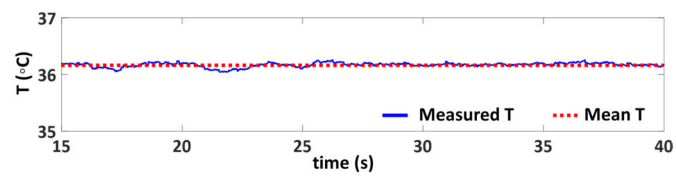


Fig. 17. Measured skin temperature curve.

to compare PPG waves from our system with the commercial device. Therefore, the PPG signals were used to calculate the SpO2 value with our developed SpO2 algorithm (see details in the section of Algorithms Validation). Then the calculated value was used to compare with the SpO2 value from a CE approved commercial pulse oximeter (CONTEC$^{TM}$ Pulse Oximeter, model: CMS50D).

***3) Chest Movement:*** Chest movement was measured with a tri-axial accelerometer. Fig. 15 shows chest movement with respiratory expansion and coughing. The periodic respiratory movement is clearly visible in Fig. 15(a), whereas in Fig. 15(b) the cough-induced movement dominates the respiratory movement.

***4) Coughing Signal:*** The analog signal from the audio-based monitoring module was used to measure and analyze the acoustic properties of cough such as cough frequency, intensity and patterns. In order to validate its function, a respirologist mimicked different types of coughing activities, which were measured with the acoustic sensor. Fig. 16 shows examples of different cough signals.

***5) Body Temperature:*** Skin temperature was measured while keeping the device mounted on the chest. Fig. 17 shows the skin temperature curve obtained from the device. The readings from a commercial thermometer (KAZ thermometer, model: V901G-CAN) was 36.2°C, which is the same value with the measurement from the prototype of monitoring system.

## B. Algorithm Validation

The computing platform was validated using data measured from healthy volunteers as well as from publicly available datasets such as the BIDMC PPG and Respiration Dataset (Beth Israel Deaconess Medical Centre, Boston) [12],[13] and Capnobase [14], as appropriate.

Synchronized ECG and PPG signals are obtained from the chest and fingertips, respectively, while the subjects are at rest. These signals were typically twenty seconds to one minute in length. SpO2 and heart rate measurements were also obtained using a commercial pulse oximeter (CONTEC$^{TM}$ Pulse Oximeter, model: CMS50D). Reference blood pressure measurements were taken using a cuff-based device (Omron Blood Pressure Monitor, model: BP769CAN) after the ECG and PPG measurements as a reference for systolic and diastolic blood pressure. The protocol followed for the blood pressure measurements are in accordance with ANSI/AAMI/ISO standards [114],[115], with an adequate resting period of 10-15 minutes at room temperature, and measurements taken over bare skin. The subjects were seated on a chair with a supportive back and feet flat on the floor, with the designated arm rested on a table, ensuring the cuff is at heart level.

***1) Heart Rate:*** A total of 26 ECG data samples with reference measured heart rates were used for the validation of heart rate. Validation was performed for data from both lab subjects and online databases including a subset of the MIMIC II database and a subset of MIMIC III [13]. The mean absolute error in HR was calculated to be 1.02 bpm, with a standard deviation of 2.25 bpm.

***2) Oxygen Saturation:*** SpO2 was calculated from the dual wavelength PPG sensor worn by three different subjects in the lab over five distinct data samples and compared to the reference values obtained with commercial pulse oximeter (CONTEC$^{TM}$ Pulse Oximeter, model: CMS50D). The mean absolute error was calculated to be 1.09% with a standard deviation of 0.77% that is within the error limit ($\pm$2%) of most commercial pulse oximeters [116].

Authorized licensed use limited to: IEEE Xplore. Downloaded on October 07,2024 at 02:11:10 UTC from IEEE Xplore. Restrictions apply.

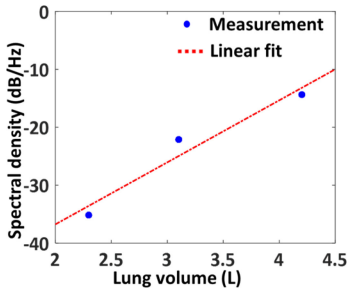


Fig. 18. Relationship between measured lung volume and spectral density of the signal from chest-mounted accelerometer.

***3) Blood Pressure:*** Blood pressure was measured for each volunteer using a cuff-based device following a strict protocol, as previously mentioned. The average of 3 subsequent measurements for SBP and DBP was used as the reference value, while the initial measurement was used for one-point PTT-BP calibration. The BIDMC and MIMIC III databases allowed for more accurate validation since continuous SBP and DBP signals can be used as the ground truth rather than discrete cuff-based BP measurements performed in earlier cases. A total of 22 synchronized ECG, PPG, and BP measurements were thus obtained both from the volunteers and publicly available databases. The mean absolute error (MAE) $\pm$ standard deviation from all sources was $3.41 \pm 2.17$ mmHg and $1.61 \pm 1.49$ mmHg for SBP and DBP, respectively. This result satisfies the clinical standards of a BP monitor that considers an MAE of $< 5$ mmHg and standard deviation of $< 8$ mmHg acceptable with respect to a reference cuff-based sphygmomanometer device [117].

***4) Respiratory Rate:*** Respiratory rate estimations were purely validated from the online public dataset, Capnobase [14]. A total of 28 synchronized ECG, PPG, and reference $CO_2$ signals were used, all of which are continuous 8-minute time samples. The MAE of the respiratory rate estimated based on ECG-derived waveforms was 0.62 breaths per minute, with a standard deviation of 2.17 breaths per minute, when compared to the reference $CO_2$ signals.

***5) Lung Volume:*** In order to show the feasibility of a chest-mounted accelerometer to estimate the lung volume, the motion data from a chest-mounted accelerometer and measurements from a clinical spirometer were obtained simultaneously under the supervision of an expert respirologist. The spectral density of the accelerometer signal showed a linear relationship with the amount of air inhaled. Fig. 18 shows one example of the relationship between the spectral density of the accelerometer signal and the lung volume. This observation may potentially enable estimating lung volume using a simple, low-cost, and wearable sensor like an accelerometer. In addition, information from the PPG signal can be fused with the accelerometer data by exploiting AI techniques to further improve the estimation accuracy that we aim to explore in future.

### *C. Performance Comparison*

Several portable and wireless multi-parameter monitoring systems are currently available in the market. However, they are not capable of monitoring a comprehensive list of parameters that may prove to be important for monitoring COVID-19 patients or patients with chronic diseases. The HR obtained from the proposed device is accurate within 1.02 bpm, which is comparable to the accuracy (errors $<1$ bpm) of the CARESCAPE One monitoring device [118]. The other commercial devices typically had MAEs within 1-3 bpm. In addition, a MAE of 0.62 breaths per minute was obtained for the respiratory rate, whereas most of the existing devices typically have errors between 1 and 2 breaths per minute.

Our estimated SpO2 is accurate within 1.09%, which is better than the Philips IntelliVue MX800 [119], which has an accuracy within $\pm 2\%$ at rest. Other commercial monitoring devices were typically accurate within $\pm$ 2-3%, while commercial pulse oximeters have mean absolute errors $<2\%$. Furthermore, the SBP and DBP estimations had mean absolute errors of 3.41 mmHg and 1.61 mmHg, respectively that showed comparable performance to existing devices [117]. Nevertheless, the performance of the proposed device requires rigorous validation on a much larger group of people including patients. Table IV presents a comparison between several state-of-the-art health monitoring systems, including the proposed one.

## VI. PERSPECTIVES AND RESEARCH CHALLENGES

As COVID-19 is a novel disease, the mitigation of the pandemic and care of patients currently poses several challenges due to the limited understanding of disease progression, current monitoring abilities and treatment options. With continuing improvement of the understanding of the virus in addition to the development of new technologies, the care of patients can largely be ameliorated. Currently, health information of COVID-19 patients is mainly recorded after the confirmation of infection and information regarding the health of patients prior to being infected with COVID-19 is largely not known. Having a device that can measure physiological parameters prior to the onset of disease can be beneficial to healthcare workers and individuals to monitor symptoms more accurately, and thus take preventative measures earlier to prevent transmission.

Information collected over the long-term (both prior to and after infection) can also allow for more accurate comparisons between infected and non-infected individuals. This would be especially useful for individuals who may be pre-symptomatic or have minor symptoms not noticeable when outwardly self-monitoring. This information will also be beneficial for allocating resources and monitoring trends to prepare for increases in cases.

A monitoring device with multiple sensors also allows the system to compensate for missing information from a faulty, damaged or disconnected sensor(s) and still provide reasonably accurate medical information. In addition, the integration of various sensors to provide information regarding several physiological parameters can allow for medical professionals to provide more specific care to individuals, particularly in the case of multiple organs being affected (as detected by a monitoring device). Having this additional information can also allow for

Authorized licensed use limited to: IEEE Xplore. Downloaded on October 07,2024 at 02:11:10 UTC from IEEE Xplore. Restrictions apply.

TABLE IV
PERFORMANCE OF THE PROPOSED DEVICE COMPARED TO COMMERCIAL DEVICES

| Ref. (Year) | System | Mounting site(s) | Description | Monitored signals and type | Performance and Accuracy |
|---|---|---|---|---|---|
| [120] (2009) | Infinity® Acute Care System, *Dräger (Germany)* | Various sites | Clinical system designed for vital-signs monitoring | • BP (IBP, NIBP)<br>• ECG: HR<br>• RR<br>• SpO2<br>• T | • Continuous monitoring<br>• Fs: 250 Hz<br>• HR: ±1% or ±2 bpm (whichever is greater) • RR: ±1 breath/min, or ±2% (whichever is greater) • NIBP: ±3 mmHg (±0.4 kPa) • T: ±0.1°C (±0.2°F) |
| [121] (2010) | IntelliVue MX800, *Philips (Netherlands)* | Various sites | Clinical system designed for vital-signs monitoring | • BP (IBP, NIBP)<br>• ECG: HR<br>• RR<br>• SpO2<br>• T | • Continuous monitoring • Fs: 4 Hz<br>• HR: ±1% of range (15-300 bpm) = ±2.85 bpm • RR: 0-120:±1 breath/min 120 - 170: ±2 breaths/min •SpO2: ±2% or ±3% depending on module •NIBP: max. Std.: 8 mmHg, max. mean error: ±5 mmHg •T: ±0.1°C (±0.2°F) |
| [122] (2013) | Hexoskin Pro Kit, *Hexoskin (Carré Technologies Inc., Canada)* | Chest | Wearable and lightweight shirt and transmitter device that can measure various physiological parameters | • HR, HRV<br>• RR • SpO2<br>• Tidal volume<br>• Minute ventilation<br>• VO2 max<br>• Activity: steps, intensity, acceleration | • Continuous monitoring<br>• Fs: 256 Hz, 12 bits (ECG)<br>• Fs: 128 Hz, 16 bits (RIP)<br>• Fs: 64Hz, 13 bits (Accelerometer)<br>• MAPE of <1% for both HR and RR from clinical study (https://www.nrcresearchpress.com/doi/abs/10.1139/apnm-2015-0140) |
| [123] (2014) | Connex® Vital signsMonitor 6000 Series, *Welch Allyn (USA)* | Various sites | Clinical system capable of vital signs, and SpO2 monitoring | • BP (IBP, NIBP)<br>• HR<br>• RR<br>• SpO2<br>• T<br>• ETCO2 | • Spot-check and continuous monitoring<br>• HR: ±3 bpm or ±3%, whichever is greater • RR: ±2 breaths per minute or ±2%, whichever is greater • NIBP: SBP: ±0.9 mmHg, DBP: ±2.2 mmHg • Clinical Masimo® or Nellcor® SpO2 measurements • T: ±0.2 °C (±0.4 °F) |
| [124] (2016) | Equivital™ EQ02+ LifeMonitor, *Hidalgo Equivital Ltd. (England)* | Chest (two shoulder strap belt) | Measurement of parameters including vital-signs, posture and motion detection | • HR • RR • T<br>• BP* • SpO2*<br>• Posture, motion, and fall detection<br>*measured using ancillary sensor | • Continuous monitoring<br>• Fs: 256 Hz, 10 bit (ECG)<br>• Fs: 25.6 Hz, 10 bit (RR)<br>• Fs: 25.6 Hz or 256 Hz - 12 bit (Accelerometer)<br>• Clinical grade (FDA approved)<br>• T: ±0.3 °C using IR thermometer |
| [127] (2017) | Everion®, Biovotion AG (Switzerland) | Upper arm | Comfortable, wearable armband device for measuring vital-signs and body movement | • HR, HRV ( through PPG analysis)<br>• T • RR<br>• SpO2<br>• Motion: steps, intensity | • Cont. (<12h intervals for max comfort)<br>• HR and SpO2 clinically validated<br>• HR: MAD ±4 bpm<br>• SpO2: 90-100%: ±3% <90%: ±4%<br>• Skin T: ±1°C • RR requires complete rest<br>• HRV and SpO2 is tolerant to little motion |
| [128] (2018) | CARESCAPE ONE, *GE Healthcare (USA)* | Various sites | Clinical monitoring system with plug and play medical USB module sensors | • BP (IBP and NIBP)<br>• ECG: HR, RR<br>• SpO2<br>• Temperature<br>• Gas exchange, CO2 | • Spot-check and continuous monitoring • Fs:500 Hz (ECG)<br>• HR: ±1% or ±1 bpm, whichever is greater • RR: ±1 bpm for 0-120 bpm, ±3 bpm for 121-200 bpm • SpO2 (TruSignal): ±2% ( ±3% with motion)<br>• NIBP: ±2% or ±3 mmHg, whichever is greater • T: ±0.2°C (±0.4°F) or ±0.3°C (±0.5°F) depending on the probe used |
| [129] (2019) | VTLAB, *VitalTracer Ltd. (Canada)* | Wrist | Wearable smartwatch | • BP • HR • SpO2 • T<br>• Fall detection<br>• Step count | • Continuous monitoring |
| [130] (2019) | Biobeat BB-613WP, *Biobeat Technologies (Israel)* | Wrist and chest (either or both) | • Chest patch for disposable short term single patient use.<br>• Rechargeable smartwatch for long-term usage | • Mean arterial pressure<br>• SpO2 • T • HR, HRV<br>• SV, CO, CI, PP<br>• RR • Steps<br>• ECG: chest patch only<br>• BP (with reference BP monitor) | • Spot-check and continuous monitoring<br>• Fs: 128 Hz<br>• HR: ±3 bpm, HRV: ±2% • BP: ±3 mmHg or ±2% of reading (whichever is greater) • Pulse pressure (PP): ±5% (mmHg)<br>• Stroke volume (SV): ±5% (mL/beat) • Cardiac Output (CO): ±10% (L/min) • Cardiac Index(CI): ±10% (L/min) • SpO2: ±3% • Skin T: ±0.3°C • RR: ±2% breaths per min |
| [131] (2019) | BioSticker™ (BIOST0208, *BioIntelliSense Inc. (USA* | Chest | Wearable chest-based device | • HR • RR • T<br>• Steps, falls<br>• Sneezing and vomiting frequency<br>• Frequency and intensity of cough | • Continuous monitoring<br>• HR: < ±5 bpm • RR: 10-30 range: MAE of < 3 breaths/min. 4-42 range: MAE of < 1.5 breaths/min. • Skin T: Complies with ASTM E1112 |
| Our work | | Chest | Wearable chest-based device vital signs, and cough monitoring | • ECG: HR, HRV<br>• RR • BP • SpO2<br>• T • Frequency and intensity of cough<br>• Lung capacity and function | • Continuous monitoring<br>• Fs: 200 Hz (ECG and PPG)<br>• HR: 1.02 ± 2.25 bpm<br>• SpO2: 1.09 ± 0.77 %<br>• SBP: 3.41 ± 2.17 mmHg, DBP: 1.61 ± 1.49 mmHg<br>• RR: 0.62 ± 2.17 breaths/ min |

medical professionals to have a comprehensive understanding of their patients' health.

The pandemic comes with an additional challenge that limits access to regular healthcare services for the elderly and patients with cardiac and respiratory diseases due to visitor restrictions imposed by the healthcare facilities. However, the existing systems also limit the ability to assess patients with cardiac and respiratory disease remotely on a more regular or continuous basis [132],[133] that otherwise may help to identify, predict, and monitor cardiovascular and respiratory problems

Authorized licensed use limited to: IEEE Xplore. Downloaded on October 07,2024 at 02:11:10 UTC from IEEE Xplore. Restrictions apply.

remotely. Respiratory monitoring tools such as peak flow meters are generally used to measure peak expiratory flow rates (PEFR). However, its utility has been questioned, particularly with low completion rates. Although mini-spirometry devices and impedance oscillometry are available for in-home use, they are, however, not routinely used due to their limited accuracy. Furthermore, the bulky system used for cardiovascular health monitoring are often obtrusive, prohibitive, and impractical for regular in-home use, requiring patients to visit medical facilities frequently. Therefore, there remains an unmet need for a portable system to accurately quantify symptoms of cardiovascular and respiratory diseases, and deterioration in cardiac and lung physiology and functional capacity outside the hospital setting. Such devices can potentially allow identifying at-risk populations and closer monitoring for deteriorating patients outside the hospital setting.

Furthermore, creating user-friendly technologies can allow users to easily understand data collected about their health, and allows for medical professionals to easily adapt to, use and understand different devices and the information they provide. Increasing the ease of use can also increase the likelihood that individuals will continue to use monitoring devices for a longer timeframe, which ultimately improves the understanding of physiological parameters of COVID-19 patients and non-infected individuals.

A fully integrated compact wearable monitoring system is therefore indispensable for enabling in-home monitoring of patients of COVID-19 and other chronic diseases. The successful implementation of the proof-of-concept wearable monitoring device thus enables us to develop a fully integrated compact wearable monitoring system in future. Such a system may comprise of two parts – a disposable part, which includes 2 commercial Ag/AgCl ECG electrodes and a reusable part that includes the waterproof and disinfectable enclosure, main circuit board, a rechargeable battery and a reusable patch with two female-type snap buttons to collect ECG signals from the ECG electrodes. The main circuit board contain the accelerometer, interface for the microphone, the PPG sensor, temperature sensor, the BLE module and a microcontroller.

The PPG sensor and the temperature sensor will be exposed and in contact to the skin through the openings made on the lead of the enclosure, the reusable patch, and the disposable patch. The enclosure will be made water resistant (Ingress Protection: IP67) with a double-sided adhesive gasket, similar to the waterproof cell phones. In addition, we aim to make use of the concept of sensor fusion to estimate the lung functions and lung capacity using the information obtained from different sensors. However, the accuracy of the sensor fusion technique can be affected if the signals from different sensors are not synchronized. For example, in the case of cuffless BP estimation, BP is estimated from the PTT. Therefore, proper time-synchronization is required between ECG and PPG waveforms to ensure accurate calculation of PTT, and BP, thereby.

In addition, the data from the accelerometer, which is used to sense the chest movement, can be fused with the acoustic signal from the microphone to enhance the accuracy of the audio-based cough monitoring. The accelerometer data can also be used to estimate and correct for motion artifacts to increase the quality of the ECG and PPG signals. Therefore, the accelerometer also needs to be time-synchronized with other sensors. To address this issue, a synchronized global clock can be used to sample the signals from all sensors. Alternately, the global clock can be used to insert timestamps for each signal that will allow processing the data from different sensors by using their timing information. Fig. 19 presents the diagram of a fully integrated compact wearable health monitoring system.

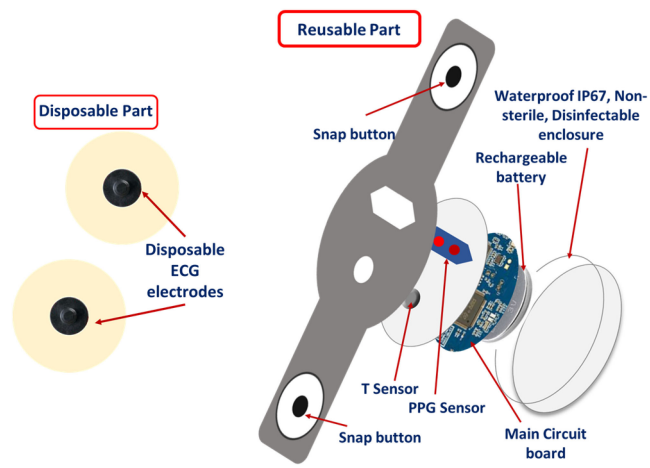


Fig. 19. A fully integrated compact wearable health monitoring system.

Another important issue for the wearable device is the lifetime of the battery after one charge. Since the suggested quarantine time for a COVID-19 patient is 14 days, a minimum 14-day lifetime for the battery of the COVID-19 monitoring system is necessary to enable continuous and uninterrupted monitoring after one full charge cycle. Therefore, the power requirements of the signal conditioning and processing circuits of the system should also be taken into the consideration at the initial stage of component selections. Some other controlling techniques can also be employed. For example, the system can be designed to have different operation modes such as sleep mode, normal mode, and active mode. Each mode will run at different data sampling clocks and different data acquisition frequencies. Based on the lung function of the patient, the system can automatically enter different operation modes. If the lung function of the patient is improving, the data acquisition frequency can be reduced. On the contrary, if the lung function deteriorates, the data acquisition frequency can be increased. Wireless charging techniques or energy harvesting techniques can potentially be used to enhance the operating time of the system to enable continuous monitoring for a long period of time.

## VII. CONCLUSION

Although preventative measures to reduce the spread of the SARS-CoV-2 currently exist, improved methods of symptom monitoring can largely reduce the community spread of the virus, in addition to enhancing the monitoring of general physical health. Accurate monitoring of physiological parameters without the need for periodic testing or frequent hospital visits is highly beneficial, especially during the COVID-19 pandemic. The cardiovascular system and respiratory system are both

Authorized licensed use limited to: IEEE Xplore. Downloaded on October 07,2024 at 02:11:10 UTC from IEEE Xplore. Restrictions apply.

complex, integrated and are implicated in several diseases. The cardiovascular system is an integral part of the transport of oxygen, nutrients, and by-products of metabolism. Failure of this mechanism leads to acute or chronic heart failure. Symptoms of chest pain, palpitations, shortness of breath, fatigue and chest tightness are possible symptoms suggesting an increase in the workload presented. This may be due to an impairment in cardiac contractility, reduced blood supply or oxygenation to the myocardium and/or vascular disease. Furthermore, respiratory physiology maintains homeostasis, providing oxygen uptake and carbon dioxide elimination from the body. If this equilibrium is not properly maintained, respiratory failure may result. Symptoms of cough, shortness of breath, wheeze and chest tightness are the body's way of alerting patients of an increased workload, by either an acute infection or an impairment in the muscles of respiration, airway obstruction, vascular disease, and/or alveolar gas exchange. Having an improved understanding of one's physical health may also improve mental well-being, by decreasing anxiety surrounding one's health condition. To date, there exists several monitoring devices that assist with the identification, prediction and monitoring of acute and chronic heart diseases and respiratory diseases. The use of simple, wearable, non-obtrusive sensor devices with remote monitoring can reduce hospital visits and admissions. Advances in engineering coupled with a simple, easy to use design in an outpatient setting is the way of the future. In conclusion, the proposed device showed promising results in this preliminary stage of development with good compliance to the clinical standards for measuring a variety of parameters including heart rate, saturated blood oxygen levels, systolic and diastolic blood pressure, respiratory rate and lung volume. The device is able to collect all of these signals using a simple, wearable chest-based device, which allows for flexibility and comfort not found in many existing commercial devices, spanning both consumer-based and clinical models. By accurately and remotely monitoring several physiological parameters in a user-friendly manner, this device holds great promise for ameliorating healthcare. Nevertheless, the performance of the proposed device must be validated on a much larger and diverse group of people including patients that we plan to address in our future work.

## References


[1] Johns Hopkins University Medicine, *Coronavirus Resource Center - By Region*. Baltimore, MD, USA: Johns Hopkins Univ. of Medicine, Oct. 2021.

[2] United Nations, Department of Economic and Social Affairs, *World Population Prospects 2019*, New York, NY, USA, Jul. 1, 2020, Accessed: Apr. 17, 2021. [Online]. Available: https://population.un.org/wpp/Download/Standard/Population/

[3] Centers for Disease Control and Prevention, "Hospitalization rates and characteristics of patients hospitalized with laboratory-confirmed coronavirus disease 2019 - COVID-NET, 14 states, March 1–30, 2020," Apr. 2020. [Online]. Available: https://www.cdc.gov/mmwr/volumes/69/wr/mm6915e3.htm

[4] G. Grasselli, A. Pesenti, and M. Cecconi, "Critical care utilization for the COVID-19 outbreak in Lombardy, Italy: Early experience and forecast during an emergency response," *JAMA,* vol. 323, no. 16, pp. 1545–1546, 2020.

[5] A. Remuzzi and G. Remuzzi, "COVID-19 and Italy: What next?," *Lancet*, vol. 395, no. 10231, pp. 1225–1228, 2020.

[6] J. Zhu *et al.*, "Clinical characteristics of 3062 COVID-19 patients: A meta-analysis," *J. Med. Virol.*, vol. 92, no. 10, pp. 1902–1914, 2020.

[7] M. G. Argenzian *et al.*, "Characterization and clinical course of 1000 patients with coronavirus disease 2019 in New York: Retrospective case series," *BMJ*, vol. 369, 2020, Art. no. m1996.

[8] H. Jeong, J. A. Rogers, and S. Xu, "Continuous on-body sensing for the COVID-19 pandemic: Gaps and opportunities," *Sci. Adv.*, vol. 6, no. 36, 2020, Art. no. eabd4794.

[9] D. R. Seshadri *et al.*, "Wearable sensors for COVID-19: A call to action to harness our digital infrastructure for remote patient monitoring and virtual assessments," *Front. Digit. Health.*, vol. 2, 2020, Art. no. 8.

[10] G. Quer *et al.*, "Wearable sensor data and self-reported symptoms for COVID-19 detection," *Nat. Med.*, vol. 27, no. 1, pp. 73–77, 2020.

[11] X. R. Ding *et al.*, "Wearable sensing and telehealth technology with potential applications in the coronavirus pandemic," *IEEE Rev. Biomed. Eng.*, vol. 14, pp. 48–70, May 2020.

[12] "BIDMC PPG and respiration dataset," *BIDMC PPG Respiration Dataset v1.0.0*, Jun. 2018. [Online]. Available: https://physionet.org/content/bidmc/1.0.0/

[13] B. Moody, G. Moody, M. Villarroel, G. Clifford, and I. Silva, "MIMIC-III waveform database matched subset," *MIMIC-III Waveform Database Matched Subset v1.0*, Apr. 2020. [Online]. Available: https://www.physionet.org/content/mimic3wdb-matched/1.0/

[14] W. Karlen, "CapnoBase," in *CapnoBase.org: Pulse Oximeter IEEE TBME Benchmark*. Nov. 2014. [Online]. Available: http://www.capnobase.org/index.php?id=857

[15] Y. Yang, W. Shang, and X. Rao, "Facing the COVID-19 outbreak: What should we know and what could we do?," *J. Med. Virol.*, vol. 92, no. 6, pp. 536–537, 2020.

[16] P. Pokhrel, C. Hu, and H. Mao, "Detecting the coronavirus (COVID-19)," *ACS Sensors*, vol. 5, no. 8. pp. 2283–2297, 2020.

[17] L. Morawska and J. Cao, "Airborne transmission of SARS-CoV-2: The world should face the reality," *Environ. Int.*, vol. 139, 2020, Art. no. 105730.

[18] N. J. Matheson and P. J. Lehner, "How does SARS-CoV-2 cause COVID-19?," *Science,* vol. 369, no. 6503, pp. 510–511, 2020.

[19] J. Shang *et al.*, "Cell entry mechanisms of SARS-CoV-2," *Proc. Nat. Acad. Sci.*, vol. 117, no. 21, pp. 11727–11734, 2020.

[20] John Hopkins Medicine, "How coronaviruses work," Jul. 22, 2020, Accessed: Sep. 21, 2020. [Online]. Available: https://www.youtube.com/watch?v=oCelMyMtRCk

[21] S. Richardson, J. S. Hirsch, and M. Narasimhan, "Presenting characteristics, comorbidities, and outcomes among 5700 patients hospitalized with COVID-19 in the New York City area," *J. Amer. Med. Assoc.,* vol. 323, no. 20, pp. 2052–2059, 2020.

[22] Centers for Disease Control and Prevention, "Interim clinical guidance for management of patients with confirmed coronavirus disease (COVID-19)," Sep. 2020. [Online]. Available: https://www.cdc.gov/coronavirus/2019-ncov/hcp/clinical-guidance-management-patients.html

[23] H. Nishiura and T. Kobayashi, "Estimation of the asymptomatic ratio of novel coronavirus infections (COVID-19)," *Int. J. Infect. Dis.,* vol. 94, pp. 154–155, 2020.

[24] Centers for Disease Control and Prevention, "People with certain medical conditions," Sep. 2020. [Online]. Available: https://www.cdc.gov/coronavirus/2019-ncov/need-extra-precautions/people-with-medical-conditions.html

[25] Centers for Disease Control and Prevention, "Assessing risk factors for severe COVID-19 illness," Aug. 2020, Accessed: Sep. 28, 2020. [Online]. Available: https://www.cdc.gov/coronavirus/2019-ncov/covid-data/investigations-discovery/assessing-risk-factors.html

[26] P. Cain, "What the coronavirus reproduction is, and why we should keep an eye on it," Global News, May 2020, Accessed: Sep. 28, 2020. [Online]. Available: https://globalnews.ca/news/6917781/coronavirus-reproduction-number-canada/

[27] A. Pan, L. Liu, and C. Wang, "Association of public health interventions with the epidemiology of the COVID-10 outbreak in Wuhan, China," *J. Amer. Med. Assoc.,* vol. 323, no. 19, pp. 1915–1923, 2020.

[28] D. Gunzler and A. R. Sehgal, "Time-varying COVID-19 reproduction number in the United States," Apr. 2020, Accessed: Sep. 28, 2020. [Online]. Available: https://www.medrxiv.org/content/10.1101/2020.04.10.20060863v1.full.pdf+html

[29] D. Kanduc and Y. Shoenfeld, "On the molecular determinants of the SARS-CoV-2 attack," *Clin. Immunol.,* vol. 215, 2020, Art. no. 108426.

[30] C. Robba, D. Battaglini, P. Pelosi, and P. R. M. Rocco, "Multiple organ dysfunction in SARS-CoV-2: MODS-CoV-2," *Expert Rev. Respir. Med.,* vol. 14, no. 9, pp. 865–868, 2020.


Authorized licensed use limited to: IEEE Xplore. Downloaded on October 07,2024 at 02:11:10 UTC from IEEE Xplore. Restrictions apply.

[31] A. Prasad and M. Prasad, "Single virus targeting multiple organs: What we know and where we are heading?," *Front. Med.,* vol. 7, 2020.

[32] Harvard University, *COVID-19 Basics*. Harvard, MA, USA: Harvard Health Publ., Mar. 2020. Accessed: Sep. 20, 2020. [Online]. Available: https://www.health.harvard.edu/diseases-and-conditions/covid-19-basics

[33] V. Kaminskyy and B. Zhivotovsky, "To kill or be killed: How viruses interact with the cell death machinery," *J. Intern. Med.,* vol. 267, no. 5, pp. 473–482, 2010.

[34] J. Yang *et al.*, "Prevalence of comorbidities and its effects in patients infected with SARS-CoV-2: A systematic review and meta-analysis," *Int. J. Infect. Dis.*, vol. 94, pp. 91–95, 2020.

[35] A. C. Shaw, D. R. Goldstein, and R. R. Montgomery, "Age-dependent dysregulation of innate immunity," *Nat. Rev. Immunol.*, vol. 13, no. 12, pp. 875–887, 2013.

[36] A. Lala *et al.*, "Prevalence and impact of myocardial injury in patients hospitalized with COVID-19 infection," *J. Amer. College Cardiol.*, vol. 76, no. 5, pp. 533–546, 2020.

[37] R. B. Azevedo *et al.*, "COVID-19 and the cardiovascular system: A comprehensive review," *J. Hum. Hypertension*, vol. 35, pp. 4–11, 2020.

[38] M. Ahmed *et al.*, "Multisystem inflammatory syndrome in children: A systematic review," *EClin. Med.*, vol. 26, 2020, Art. no. 100527.

[39] V. O. Puntmann *et al.*, "Outcomes of cardiovascular magnetic resonance imaging in patients recently recovered from coronavirus disease 2019 (COVID-19)," *JAMA Cardiol.*, vol. 5, no. 11, pp. 1265–1273, 2020.

[40] N. Mangalmurti and C. A. Hunter, "Cytokine storms: Understanding COVID-19," *Immunity*, vol. 53, no. 1, pp. 19–25, 2020.

[41] E. Driggin *et al.*, "Cardiovascular considerations for patients, health care workers, and health systems during the COVID-19 pandemic," *J. Amer. College Cardiol.*, vol. 75, no. 18, pp. 2352–2371, 2020.

[42] G. P. Bulfamante *et al.*, "Evidence of SARS-CoV-2 transcriptional activity in cardiomyocytes of COVID-19 patients without clinical signs of cardiac involvement," *Biomedicines*, vol. 8, no. 12, pp. 1–13, 2020.

[43] K. Sawalha *et al.*, "Systematic review of COVID-19 related myocarditis: Insights on management and outcome," *Cardiovasc. Revascularization Med.*, vol. 23, pp. 107–113, Feb. 2021.

[44] H. Chen, M. Yang, and J. Liu, "Corticosteroids for viral myocarditis," *Cochrane Database Systematic Rev.*, no. 10, pp. 1–37, 2003.

[45] C. Wu *et al.*, "Risk factors associated with acute respiratory distress syndrome and death in patients with coronavirus disease 2019 pneumonia in Wuhan, China," *JAMA Intern. Med.*, vol. 180, no. 7, pp. 934–943, 2020.

[46] M. Ahmed *et al.*, "Multisystem inflammatory syndrome in children: A systematic review," *EClin. Med.*, vol. 26, 2020, Art. no. 100527.

[47] S. Majumder, L. Chen, O. Marinov, C. Chen, T. Mondal, and M. J. Deen, "Noncontact wearable wireless ECG systems for long-term monitoring," *IEEE Rev. Biomed. Eng.*, vol. 11, pp. 306–321, 2018.

[48] E. Nemati, M. J. Deen, and T. Mondal, "A wireless wearable ECG sensor for long-term applications," *IEEE Commun. Mag.*, vol. 50, no. 1, pp. 36–43, Jan. 2012.

[49] I. Satia, R. Cusack, J. M. Greene, P. M. O'Byrne, K. J. Killian, and N. Johnston, "Prevalence and contribution of respiratory viruses in the community to rates of emergency department visits and hospitalizations with respiratory tract infections, chronic obstructive pulmonary disease and asthma," *PLoS One,* vol. 15, 2020, Art. no. e0228544.

[50] A. Ortqvist *et al.*, "Aetiology, outcome and prognostic factors in community-acquired pneumonia requiring hospitalization," *Eur. Respir. J.,* vol. 3, pp. 1105–1113, 1990.

[51] P. Macklem, "Obstruction in small airways—A challenge to medicine," *Amer. J. Med.,* vol. 52, pp. 721–724, 1972.

[52] J. V. Fahy and B. F. Dickey, "Airway mucus function and dysfunction," *New England J. Med.,* vol. 363, pp. 2233–2247, 2010.

[53] T. Narasaraju *et al.*, "Excessive neutrophils and neutrophil extracellular traps contribute to acute lung injury of influenza pneumonitis," *Amer. J. Pathol.,* vol. 179, pp. 199–210, 2011.

[54] S. P. Galant, H. D. Komarow, H.-W. Shin, S. Siddiqui, and B. J. Lipworth, "The case for impulse oscillometry in the management of asthma in children and adults," *Ann. Allergy, Asthma Immunol.,* vol. 118, pp. 664–671, 2017.

[55] R. Tramm, D. Ilic, A. R. Davies, V. A. Pellegrino, L. Romero, and C. Hodgson, "Extracorporeal membrane oxygenation for critically ill adults," *Cochrane Database Systematic Rev.,* no. 1, pp. 1–42, 2015.

[56] P. A. Marsden *et al.*, "A comparison of objective and subjective measures of cough in asthma," *J. Allergy Clin. Immunol.,* vol. 122, no. 5, pp. 903–907, 2008.

[57] J. A. Smith *et al.*, "Gefapixant, a P2X3 receptor antagonist, for the treatment of refractory or unexplained chronic cough: A randomised, double-blind, controlled, parallel-group, phase 2b trial," *Lancet Respir. Med.,* vol. 8, no. 8, pp. 775–785, 2020.

[58] R. J. Khusial *et al.*, "Effectiveness of myAirCoach: A mHealth self-management system in asthma," *J. Allergy Clin. Immunol.: Pract.,* vol. 8, no. 6, pp. 1972–1979.e8, 2020.

[59] P. J. Honkoop *et al.*, "MyAirCoach: The use of home-monitoring and mHealth systems to predict deterioration in asthma control and the occurrence of asthma exacerbations; study protocol of an observational study," *BMJ Open,* vol. 7, no. 1, 2017, Art. no. e013935.

[60] R. P. Rajkumar, "COVID-19 and mental health: A review of the existing literature," *Asian J. Psychiatry*, vol. 52, 2020, Art. no. 102066.

[61] D. Roy, S. Tripathy, S. K. Kar, N. Sharma, S. K. Verma, and V. Kaushal, "Study of knowledge, attitude, anxiety & perceived mental healthcare need in T Indian population during COVID-19 pandemic," *Asian J. Psychiatry,* vol. 51, 2020, Art. no. 102083.

[62] B. Pfefferbaum and C. S. North, "Mental health and the COVID-19 pandemic," *New England J. Med.,* vol. 383, no. 6, pp. 510–512, 2020.

[63] G. J. Asmundson, M. M. Paluszek, C. A. Landry, G. S. Rachor, D. McKay, and S. Taylor, "Do pre-existing anxiety-related and mood disorders differentially impact COVID-19 stress responses and coping?," *J. Anxiety Disord.,* vol. 74, 2020, Art. no. 102271.

[64] D. Horesh, R. K. Lev-Ari, and I. Hasson-Ohayon, "Risk factors for psychological distress during the COVID-19 pandemic in Israel: Loneliness, age, gender, and health status play an important role," *Brit. J. Health Psychol.,* vol. 25, no. 4, pp. 925–933, 2020.

[65] World Health Organization, "COVID-19 strategy update," Apr. 2020. Accessed: Sep. 21, 2020. [Online]. Available: https://www.who.int/publications/i/item/strategic-preparedness-and-response-plan-for-the-new-coronavirus

[66] A. Pan *et al.*, "Association of public health interventions with the epidemiology of the COVID-19 outbreak in Wuhan, China," *J. Amer. Med. Assoc.,* vol. 323, no. 19, pp. 1915–1923, 2020.

[67] S. Gupta *et al.*, "Tracking public and private responses to the COVID-19 epidemic: Evidence from state and local government actions," *Nat. Bur. Econ. Res.,* 2020, Art. no. 27027.

[68] S. Majumder, T. Mondal, and M. Deen, "Wearable sensors for remote health monitoring," *Sensors*, vol. 17, no. 12, pp. 1–44, 2017.

[69] M. J. Deen, "Information and communications technologies for elderly ubiquitous healthcare in a smart home," *Pers. Ubiquitous Comput.*, vol. 19, no. 3, pp. 573–599, 2015.

[70] S. Majumder *et al.*, "Smart homes for elderly healthcare—Recent advances and research challenges," *Sensors*, vol. 17, no. 11, pp. 2496–2527, 2017.

[71] B. Jin *et al.*, "Walking-age analyzer for healthcare applications," *IEEE J. Biomed. Health Inform.*, vol. 18, no. 3, pp. 1034–1042, May 2014.

[72] P. Mandal, K. Tank, T. Mondal, C. H. Chen, and M. J. Deen, "Predictive walking-age health analyzer," *IEEE J. Biomed. Health Inform.*, vol. 22, no. 2, pp. 363–374, Mar. 2018.

[73] S. Majumder and M. J. Deen, "A robust orientation filter for wearable sensing applications," *IEEE Sensors J.*, vol. 20, no. 23, pp. 14228–14236, Dec. 2020.

[74] S. Majumder, T. Mondal, and M. J. Deen, "A simple, low–cost and efficient gait analyzer for wearable healthcare applications," *IEEE Sensors J.*, vol. 19, no. 6, pp. 2320–2329, Mar. 2019.

[75] S. Majumder and M. J. Deen, "Wearable IMU-based system for real-time monitoring of lower-limb joints," *IEEE Sensors J.*, vol. 21, no. 6, pp. 8267–8275, Mar. 2021.

[76] A. I. Faisal, S. Majumder, R. Scott, T. Mondal, D. Cowan, and M. J. Deen, "A simple, low-cost multi-sensor-based smart wearable knee monitoring system," *IEEE Sensors J.*, vol. 21, no. 6, pp. 8253–8266, Mar. 2021.

[77] A. I. Faisal, S. Majumder, T. Mondal, D. Cowan, S. Naseh, and M. J. Deen, "Monitoring methods of human body joints: State-of-the-art and research challenges," *Sensors*, vol. 19, no. 11, 2019, Art. no. 2629.

[78] S.-T. Tseng *et al.*, "A 65-nm CMOS low-power impulse radar system for human respiratory feature extraction and diagnosis on respiratory diseases," *IEEE Trans. Microw. Theory Techn.*, vol. 64, no. 4, pp. 1029–1041, Apr. 2016.

[79] X. Wang, C. Yang, and S. Mao, "PhaseBeat: Exploiting CSI phase data for vital sign monitoring with commodity WiFi devices," in *Proc. IEEE 37th Int. Conf. Distrib. Comput. Syst.*, 2017, pp. 1230–1239.


Authorized licensed use limited to: IEEE Xplore. Downloaded on October 07,2024 at 02:11:10 UTC from IEEE Xplore. Restrictions apply.

[80] I. Song, "Diagnosis of pneumonia from sounds collected using low cost cell phones," in *Proc. Int. Joint Conf. Neural Netw.*, 2015, pp. 1–8.

[81] Z. Jiang *et al.*, "Detection of respiratory infections using RGB-infrared sensors on portable device," *IEEE Sensors J.*, vol. 20, no. 22, pp. 13674–13681, Nov. 2020.

[82] X. Tang, D. K. Du, Z. He, and J. Liu, "PyramidBox: A context-assisted single shot face detector," in *Computer Vision—ECCV 2018 Lecture Notes in Computer Science*, Cham, Switzerland: Springer, 2018, pp. 812–828.

[83] A. Imran *et al.*, "AI4COVID-19: AI enabled preliminary diagnosis for COVID-19 from cough samples via an app," *Inform. Med. Unlocked*, vol. 20, 2020, Art. no. 100378.

[84] H. S. Maghded, K. Z. Ghafoor, A. S. Sadiq, K. Curran, D. B. Rawat, and K. Rabie, "A novel AI-enabled framework to diagnose coronavirus COVID-19 using smartphone embedded sensors: Design study," in *Proc. IEEE 21st Int. Conf. Inf. Reuse Integr. Data Sci.*, 2020, pp. 180–187.

[85] I. Orha and S. Oniga, "Automated system for evaluating health status," in *Proc. IEEE 19th Int. Symp. Des. Technol. Electron. Packag.*, 2013, pp. 219–222.

[86] M. M. Baig, H. Gholamhosseini, and M. J. Connolly, "Integrated vital-signs monitoring system using ubiquitous devices: Multiple physical signs detection and decision support for hospitalized older adults," in *Proc. 37th Annu. Int. Conf. IEEE Eng. Med. Biol. Soc.*, 2015, pp. 1219–1222.

[87] R. Munnoch and P. Jiang, "A personal medical device for multi-sensor, remote vital-signs collection in the elderly," in *Proc. Sci. Inf. Conf.*, 2015, pp. 1122–1131.

[88] R. Stojanovic, A. Skraba, and B. Lutovac, "A headset like wearable device to track COVID-19 symptoms," in *Proc. 9th Mediterranean Conf. Embedded Comput.*, 2020, pp. 1–4.

[89] S. S. Thomas, V. Nathan, C. Zong, K. Soundarapandian, X. Shi, and R. Jafari, "BioWatch: A noninvasive wrist-based blood pressure monitor that incorporates training techniques for posture and subject variability," *IEEE J. Biomed. Health Inform.*, vol. 20, no. 5, pp. 1291–1300, Sep. 2016.

[90] D. Jarchi, D. Salvi, C. Velardo, A. Mahdi, L. Tarassenko, and D. A. Clifton, "Estimation of HRV and $SpO_2$ from wrist-worn commercial sensors for clinical settings," in *Proc. IEEE 15th Int. Conf. Wearable Implantable Body Sensor Netw.*, 2018, pp. 144–147.

[91] S. Ahmad *et al.*, "A prototype of an integrated blood pressure and electrocardiogram device for multi-parameter physiologic monitoring," in *Proc. IEEE Instrum. Meas. Technol. Conf.*, 2010, pp. 1244–1249.

[92] I. Silva and G. B. Moody, "An open-source toolbox for analysing and processing physionet databases in MATLAB and octave," *J. Open Res. Softw.*, vol. 2, 2014, Art. no. e27.

[93] A. L. Goldberger *et al.*, "PhysioBank, physiotoolkit, and physionet," *Circulation*, vol. 101, no. 23, 2000, Art. no. e215.

[94] M. A. F. Pimentel, M. D. Santos, C. Arteta, J. S. Domingos, M. A. Maraci, and G. D. Clifford, "Respiratory rate estimation from the oscillometric waveform obtained from a non-invasive cuff-based blood pressure device," in *Proc. 36th Annu. Int. Conf. IEEE Eng. Med. Biol. Soc.*, 2014, pp. 3821–3824.

[95] A. M. Chan, N. Selvaraj, N. Ferdosi, and R. Narasimhan, "Wireless patch sensor for remote monitoring of heart rate, respiration, activity, and falls," in *Proc. 35th Annu. Int. Conf. IEEE Eng. Med. Biol. Soc.*, 2013, pp. 6115–6118.

[96] A. M. Chan, N. Ferdosi, and R. Narasimhan, "Ambulatory respiratory rate detection using ECG and a triaxial accelerometer," in *Proc. 35th Annu. Int. Conf. IEEE Eng. Med. Biol. Soc.*, 2013, pp. 4058–4061.

[97] J. Park *et al.*, "Cuffless and continuous blood pressure monitoring using a single chest-worn device," *IEEE Access*, vol. 7, pp. 135231–135246, 2019.

[98] "LMT70YFQT active," *Texas Instruments*, Accessed: Nov. 2, 2020. [Online]. Available: https://www.ti.com/store/ti/en/p/product/?p=LMT70YFQT

[99] "MAX86150 integrated photoplethysmogram and electrocardiogram bio-sensor module for mobile health," *Maxim Integrated*, Accessed: Nov. 2, 2020. [Online]. Available: https://www.maximintegrated.com/en/products/interface/sensor-interface/MAX86150.html

[100] "CMC-6027-24L100," *CUI Devices*, Accessed: Nov. 2, 2020. [Online]. Available: https://www.cuidevices.com/product/audio/microphones/electret-condenser-microphones/cmc-6027-24l100

[101] "MAX86150EVSYS evaluation system for the MAX86150," *Maxim Integrated*, Accessed: Nov. 2, 2020. [Online]. Available: https://www.maximintegrated.com/en/products/sensors/MAX86150EVSYS.html

[102] "DataLOG," in *DataLOG For Portable Datainin Acquisition and Monitoring*, Accessed: Nov. 2, 2020. [Online]. Available: https://www.biometricsltd.com/datalog.htm

[103] "MetaWearC Product Specification v1.0," MBIENTLAB INC., Accessed: Nov. 2, 2020. [Online]. Available: https://mbientlab.com/documents/MetaWearC-CPRO-PS.pdf

[104] "LMT70EVM," LMT70EVM Evaluation board | TI.com, Accessed: Nov. 2, 2020. [Online]. Available: https://www.ti.com/tool/LMT70EVM

[105] "How to design peripheral oxygen saturation ($SpO_2$) and optical heart rate monitoring (OHRM) systems using the AFE4403," *Texas Instruments*, Accessed: Feb. 26, 2021. [Online]. Available: https://www.ti.com/lit/an/slaa655/slaa655.pdf

[106] E. D. Chan, M. M. Chan, and M. M. Chan, "Pulse oximetry: Understanding its basic principles facilitates appreciation of its limitations," *Respir. Med.*, vol. 107, no. 6, pp. 789–799, 2013.

[107] R. Mukkamala *et al.*, "Toward ubiquitous blood pressure monitoring via pulse transit time: Theory and practice," *IEEE Trans. Biomed. Eng.*, vol. 62, no. 8, pp. 1879–1901, Aug. 2015.

[108] T. Wibmer *et al.*, "Pulse transit time and blood pressure during cardiopulmonary exercise tests," *Physiol. Res.*, vol. 63, no. 3, pp. 287–296, 2014.

[109] R. Wang, W. Jia, Z.-H. Mao, R. J. Sclabassi, and M. Sun, "Cuff-free blood pressure estimation using pulse transit time and heart rate," in *Proc. 12th Int. Conf. Signal Process.*, 2014, pp. 115–118.

[110] D. J. Hughes, C. F. Babbs, L. A. Geddes, and J. D. Bourland, "Measurements of Young's modulus of elasticity of the canine aorta with ultrasound," *Ultrason. Imag.*, vol. 1, no. 4, pp. 356–367, 1979.

[111] Y. Zheng, B. P. Yan, Y. Zhang, and C. C. Y. Poon, "An armband wearable device for overnight and cuff-less blood pressure measurement," *IEEE Trans. Biomed. Eng.*, vol. 61, no. 7, pp. 2179–2186, Jul. 2014.

[112] F. Yasuma and J.-I. Hayano, "Respiratory sinus arrhythmia," *Chest*, vol. 125, no. 2, pp. 683–690, 2004.

[113] L. Mirmohamadsadeghi and J.-M. Vesin, "Respiratory rate estimation from the ECG using an instantaneous frequency tracking algorithm," *Biomed. Signal Process. Control*, vol. 14, pp. 66–72, 2014.

[114] *Non-Invasive Sphygmomanometers — Part 2: Clinical Validation of Automated Measurement Type*, ANSI Standard ANSI/AAMI/ISO 81060-2, 2013. [Online]. Available: https://my.aami.org/aamiresources/previewfiles/8106002_1306_preview.pdf

[115] *Non-Invasive Sphygmomanometers — Part 2: Clinical Investigation of Intermittent Automated Measurement Type*, ISO 81060-2:2018, Nov. 21, 2018. Accessed: Nov. 2, 2020. [Online]. Available: https://www.iso.org/standard/73339.html

[116] "Pulse oximetry," *American Thoracic Society*, Accessed: Feb. 26, 2021. [Online]. Available: https://www.thoracic.org/patients/patient-resources/resources/pulse-oximetry.pdf

[117] B. Shahbabu, "Which is more accurate in measuring the blood pressure? A digital or an aneroid sphygmomanometer," *J. Clin. Diagn. Res.*, vol. 10, no. 3, pp. LC11–LC14, 2016.

[118] "CARESCAPE ONE monitoring system," *GE Healthcare*, Accessed: Feb. 26, 2021. [Online]. Available: https://www.vingmed.dk/wp-content/uploads/sites/3/2020/06/MS-Global-CARESCAPE-ONE-Spec-sheet-English-05-2018-DOC1959489-rev2.pdf

[119] "IntelliVue MX800 bedside patient monitor: Philips healthcare," *Philips*, Accessed: Feb. 26, 2021. [Online]. Available: https://www.usa.philips.com/healthcare/product/HC865240/intellivue-mx800-bedside-patient-monitor

[120] "Infinity acute care system," *Draeger*, Accessed: Feb. 26, 2021. [Online]. Available: https://www.draeger.com/en-us_ca/Hospital/Products/Patient-Monitoring/Patient-Monitors/Infinity-Acute-Care-System

[121] "IntelliVue MX800 bedside patient monitor: Philips healthcare," *Philips*, Accessed: Feb. 26, 2021. [Online]. Available: https://www.usa.philips.com/healthcare/product/HC865240/intellivue-mx800-bedside-patient-monitor

[122] Carre Technologies inc (Hexoskin). "Hexoskin smart kit - Men's," Accessed: Feb. 26, 2021. [Online]. Available: https://www.hexoskin.com/products/hexoskin-smart-kit-mens

[123] W. Allyn, "Connex vital-signsmonitor," *Canada*, Accessed: Feb. 26, 2021. [Online]. Available: http://www.welchallyn.ca/en/products/categories/patient-monitoring/vital-signs-devices/connex-vital-signs-monitor.html

[124] "The EQ02+ lifemonitor," *Equivital*, Accessed: Feb. 26, 2021. [Online]. Available: https://www.equivital.com/assets/common/EQ02+_08_Equivital_Data_Sheets_v8_(003).pdf

[125] J. Laguarta, F. Hueto, and B. Subirana, "COVID-19 artificial intelligence diagnosis using only cough recordings," *IEEE Open J. Eng. Med. Biol.*, vol. 1, pp. 275–281, Sep. 2020.

[126] M. Galarnyk, G. Quer, K. McLaughlin, L. Ariniello, and S. R. Steinhubl, "Usability of a wrist-worn smartwatch in a direct-to-participant randomized pragmatic clinical trial," *Digit. Biomarkers*, vol. 3, no. 3, pp. 176–184, 2019.


Authorized licensed use limited to: IEEE Xplore. Downloaded on October 07,2024 at 02:11:10 UTC from IEEE Xplore. Restrictions apply.

[127] "Everion device," *Everion Device – Biofourmis AG*, Accessed: Nov. 2, 2020. [Online]. Available: https://support.biofourmis.com/hc/en-us/categories/201377109-Everion-Device-
[128] "CARESCAPE ONE monitoring system," *GE Healthcare*, Accessed: Feb. 26, 2021. [Online]. Available: https://www.vingmed.dk/wp-content/uploads/sites/3/2020/06/MS-Global-CARESCAPE-ONE-Spec-sheet-English-05-2018-DOC1959489-rev2.pdf
[129] VitalTracer, "VTLAB (pre-order)," Accessed: Feb. 26, 2021. [Online]. Available: https://vitaltracer.com/product/vtlab/
[130] "Short-Term Monitoring," *Biobeat*, Accessed: Feb. 26, 2021. [Online]. Available: https://www.bio-beat.com/short-term
[131] "Medical grade COVID screening at scale," *BioIntelliSense*, Accessed: Feb. 26, 2021. [Online]. Available: https://biointellisense.com/
[132] Y. Liu *et al.*, "A novel cloud-based framework for the elderly healthcare services using digital twin," *IEEE Access*, vol. 7, pp. 49088–49101, Apr. 2019.
[133] M. Naghshvarianjahromi, S. Kumar, and M. J. Deen, "Brain-inspired intelli-gence for real-time health situation understanding in smart e-Health home applications," *IEEE Access*, vol. 7, pp. 180106–180126, Dec. 2019.

**Wei Jiang** received the B.Sc. degree in electrical and electronic engineering from Xi'an Jiaotong University, Xi'an, China, in 2006 and the M.A.Sc. degree in microelectronics from Shanghai Jiaotong University, Shanghai, China, in 2009. He is currently working toward the Ph.D. degree in biomedical engineering from McMaster University, Hamilton, ON, Canada. His current research interests include high-speed single avalanche photodiodes (SPADs), high-performance CMOS time-to-digital converters, and their applications for biomedical imaging.

**Sumit Majumder** (Graduate Student Member, IEEE) received the B.Sc. degree in electrical and electronic engineering from the Bangladesh University of Engineering and Technology, Dhaka, Bangladesh, in 2007, the M.A.Sc. in electrical and computer engineering from McMaster University, Hamilton, ON, Canada, in 2011, and the Ph.D. degree in electrical and computer engineering from McMaster University, Hamilton, ON, Canada, in 2020. He is currently a Research Engineer with the Department of Electrical and Computer Engineering, McMaster University, Hamilton, ON, Canada. His research interests include wearable sensors, biomedical signal processing, tele-health monitoring, artificial intelligence, and machine learning.

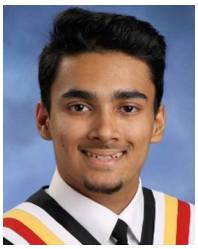

**Samarth Kumar** is currently working toward the Software and Biomedical Engineering degree with McMaster University, Hamilton, ON, Canada. His research interests include biomedical signal processing, medical imaging, and artificial intelligence.

**Sophini Subramaniam** received the H.B.Sc. degree from the University of Toronto St. George, Toronto, ON, Canada with a major in physiology and minors in immunology and french literature. She is currently working toward the M.A.Sc. degree in biomedical engineering with McMaster University, Hamilton, ON, Canada, with a focus on health monitoring using wearable sensor systems.

**Xiaohe Li** is currently an Associate Chief Physician and an Infectious Disease Specialist with the Department of Infectious Diseases, The Third People's Hospital of Shenzhen, Shenzhen, China. She has been at the forefront of treating COVID-19 patients at the top infectious diseases hospital in Shenzhen and has more than eight years experience treating patients with infectious diseases. Between March 2018 and March 2019, she was a Visiting Scholar with Stanford University, Stanford, CA, USA, conducting research in chronic liver diseases. She has authored or coauthored papers in top journals including *The Lancet Gastroenterology & Hepatology* and *Clinical Infectious Disease* on clinical interventions on COVID-19 patients.

**Ridha Khedri** is currently a Professor of software engineering with McMaster University, Hamilton, ON, Canada. His research records include more than 100 peer-reviewed papers. His current research interests include dependability and security of medical device software, algebraic methods in software engineering, information security, and ontology-based reasoning. He is a licensed Professional Engineer in the province of Ontario. He is a Member of the ACM, IEEE Computer Society, and IEEE Computer Society Technical Committee on Security and Privacy. He has been a Co-Organizer, Program Committee Member, and Referee of more than 30 international workshops and conferences.

**Tapas Mondal** has been a Pediatric Cardiologist with McMaster University, Hamilton, ON, Canada since 2005. He is currently an Associate Professor of pediatrics with McMaster University and an Associate Member with the Hospital for Sick Children, Toronto, ON, Canada, also as an Associate Member with the faculty of Engineering, McMaster University. His research interests include different imaging techniques including low-cost health monitoring systems.He was honored with the Best Teacher Award from McMaster University in 2009 (also nominated as Best teacher in 2006 and 2020) and was also the recipient of the Best Senior Resident Honor from Kalawati Saran Children's Hospital in Delhi, India. He was awarded Jeffrey Coates Award in 2018 as the first Pediatrician recipient considered to be the best physician of the city of Hamilton. He delivers integrated, personalized, family-centered patient care while creating an advanced learning environment for highly skilled personnel.

Authorized licensed use limited to: IEEE Xplore. Downloaded on October 07,2024 at 02:11:10 UTC from IEEE Xplore. Restrictions apply.

**Mansour Abolghasemian** is currently the Clinical Director with Ortho Biomed Inc. and an Assistant Professor of orthopedic surgery with Iran University of Medical Sciences, Tehran, Iran. He has more than ten years of experience in leading research projects, and currently collaborates with seven journals as an Editorial Board Member or Reviewer. He has authored or coauthored 50 peer-reviewed articles. His research interests include medical applications of artificial intelligence, wearable sensors, in addition to clinical outcome and biomechanical studies. He is currently directing multiple Research & Development projects. He was the recipient of eight research awards. He is Fellowship-trained in Hip & Pelvis Surgery from IUMS, Iran, and in Adult Reconstruction from the University of Toronto, Canada.

**Imran Satia** was born and brought up in the Blackburn, England. He graduated in medicine from the University of Cambridge, Cambridge, U.K., in 2006 with a master's in neurophysiology and started the clinical training in the North West of England. He is currently a Faculty with McMaster University, Hamilton, ON, Canada and the Firestone Institute for Respiratory Health, as an Assistant Professor of respiratory medicine. He consults on patients with refractory chronic cough, complex airways diseases and has a broad research interest in understanding the mechanisms and developing treatments for patients with chronic cough. He gained his Membership of the Royal College of Physicians (MRCP, London, U.K.) and completed his specialist training in general internal medicine and respiratory medicine. In 2017 he was awarded a Ph.D. investigating the mechanisms of cough in asthma under the supervision of world renowned cough expert Professor Jacky Smith at the University of Manchester. He was awarded the British Medical Association James Trust Award for asthma research. He recently completed a prestigious two year European Respiratory Society Respire three Marie Curie Post-Doctoral Fellowship from McMaster University to work alongside world renowned asthma expert, the Dean and Vice President of the Faculty of Health Sciences, Professor Paul O'Byrne. He was recently awarded the E.J. Moran Campbell Early Career Award

**M. Jamal Deen** (Fellow, IEEE) is currently a Distinguished University Professor, the Senior Canada Research Chair of information technology, and the Director of the Micro- and Nano-Systems Laboratory, McMaster University, Hamilton, ON, Canada. His research records include more than 620 peer-reviewed articles and two textbooks *Silicon Phonics: Fundamentals and Devices* (Wiley, 2002) and *Fiber Optic Communications: Fundamentals and Applications* (Wiley, 2014). His current research interests include nano-/opto-electronics, nanotechnology, data analytics and their emerging applications in health and environment. He was elected to Fellow status in twelve national academies and professional societies, including Royal Society of Canada, American Physical Society, Electrochemical Society and Chinese Academy of Sciences. Recently, he was elected to the Order of Canada in July 2018, the highest civilian honor awarded by the Government of Canada.

Authorized licensed use limited to: IEEE Xplore. Downloaded on October 07,2024 at 02:11:10 UTC from IEEE Xplore. Restrictions apply.